Does social rank influence AMPA receptor subunits in the medial prefrontal cortex of adult male and female rats?

by

Eden Solomon

A thesis

presented to the University of Waterloo

in fulfillment of the

thesis requirement for the degree of

Master of Science

in

Public Health Sciences

Waterloo, Ontario, Canada, 2024

© Eden Solomon 2024

Author's Declaration

I hereby declare that I am the sole author of this thesis. This is a true copy of the thesis, including any required final revisions, as accepted by my examiners.

I understand that my thesis may be made electronically available to the public.

Abstract

Introduction: Social dominance hierarchies are ubiquitously observed in social species across the animal kingdom. Social interactions, including resource competition and conflict, shape dominance structures, where animals are ranked as dominant, or subordinate to one another. Previous work has implicated the medial prefrontal cortex (mPFC) as a key brain region responsible for controlling social hierarchy through α-amino-3-hydroxy-5-methyl-4-isoxazolepropionic acid receptor (AMPA) function. The trafficking of AMPARs at the synapse plays a key role in synaptic plasticity, and is mediated by interactions between AMPARs and their associated auxiliary proteins. To date, no studies have explored the expression of AMPAR subunits and their auxiliary proteins in the context of a social hierarchy. As a result, the current study aimed to elucidate the effect that social rank might have on the most abundant AMPAR subunits, GluA1 and GluA2, along with their principal auxiliary proteins, GRIP1, PICK1, and stargazin, in both male and female rats.

Methods: Adult, 14-week old, male and female Sprague-Dawley rats were group-housed by sex in sets of four (n = 10 groups) for two weeks prior to behavioural testing. The Tube Test was then used to determine the social position of the rats, with alpha's being the most dominant, and delta animals being the least dominant. Western blotting was performed to determine the effects of social position on the expression of GluA1, GluA2, GRIP1, PICK1, and stargazin in whole cell homogenates prepared from the mPFC of these rats. A two-factor ANOVA was used to explore the effect of sex, position and their interaction on the expression of the proteins

of interest. Corticosterone levels were also analyzed to determine whether perceived stress related to social position varied across the groups and influenced neural protein expression.

Results: Social position was found to influence most of the neural proteins either independently, or through an interaction with sex. Both GluA2 ($p = .049$, $\eta^2 = .081$) and GRIP1 ($p = .012$, $\eta^2 = .095$) expression, regardless of sex, significantly differed between alpha and delta animals, where the higher ranked animals displayed increased expression of these proteins. The expression of PICK1 ($p = .047$, $\eta^2 = .011$) and stargazin ($p = .040$, $\eta^2 = .012$) were modulated through a sex by position interaction. No significant differences across sex or social position were observed with GluA1 expression. Further, while female rats exhibited approximately double the serum level of corticosterone compared to male rats, corticosterone levels did not differ across social positions.

Conclusion: The present study adds to the literature on male-male and female-female social dynamics in adult rats, and provides the first report on whether the expression of AMPAR subunits and their key regulatory proteins vary as a function of an animal's social position.

Acknowledgements

Firstly, I would like to express my deepest gratitude to my supervisor, Dr. John Mielke for his kindness, advice, and dedication to mentorship for the years that I have known him as an undergraduate student until now. I have grown so much over the past few years, and am a better scientist owing to your guidance.

To my committee members, Dr. Diane Williams and Dr. Melissa Holmes, your advice and valuable feedback have made me a better researcher. I am also extremely grateful to Dr. Reza Ramezan for his assistance with the statistical analysis. I would also like to acknowledge the funding support of the Natural Sciences and Engineering Research Council (NSERC).

To my amazing lab mates, David, Charithe, and Jugad, thank you for making long lab feel shorter, and the challenging days feel lighter. I would not be here without your encouragement. To my friends, your support has been paramount in pushing me through the past two years, trivia nights at the Grad House and coffee runs Uptown will be the memories I hold close to my heart. I especially want to thank Alicia, Nadia, and Nicole, I am so fortunate to have you in my life.

Finally to my lovely family, my parents, Danny, and Gashe, as well as my partner Patrick, how lucky am I to have a support system who loves me so much. Your unwavering support and patience have made this possible, and I will never be able to express how grateful I am. This thesis is as much yours as it is mine.

Table of Contents

Author's Declaration ..... **ii**
Abstract ..... **iii**
Acknowledgements ..... **v**
List of Figures ..... **viii**
List of Tables ..... **x**
List of Abbreviations ..... **xi**
Chapter 1 ..... **1**
Introduction **1**
1.1 Social Dominance Hierarchies 1
1.1.1 Physiological Outcome of Hierarchies 3
1.1.2 Social Stress 4
1.2 Neural Mechanisms of Social Interactions 6
1.2.1 The Social Decision-Making Network 6
1.2.2 Prefrontal-Cortical Circuits 7
1.2.3 Neurotransmitters and Hormones 9
1.3 Glutamatergic Signalling 11
1.3.1 AMPAR protein-protein interactions 13
1.3.2 AMPARs and Social Rank 14
Chapter 2 ..... **17**
Specific Aims **17**
2.1 Rationale 17
2.2 Study Objectives 17
2.3 Hypotheses 18
Chapter 3 ..... **19**
Methods **19**
3.1 Animals 19
3.2 Behavioural Experiments 19
3.3 Blood and Brain Tissue Collection 21
3.4 Synaptoneurosome Preparation 21
3.4.1 Two-step syringe-driven filtration 22
3.4.2 Spin-tube filtration 23
3.4.3 Syringe-driven filtration followed by spin-tube filtration. 24
3.5 Protein Assay 25
3.6 Quality Control Blotting of SNPs 25
3.7 Preparation of Medial Prefrontal Cortex Homogenates 25
3.8 Standard Curve Optimization 26
3.9 SDS-PAGE and Western blotting 26
3.10 Immunoblotting Data Analysis 28
3.11 Statistical Analysis 28
3.11.1 Testing assumptions of parametric tests 28

3.11.2 Immunoblotting data – Two-factor ANOVA design 29
3.11.3 Immunoblotting data – Corticosterone Analysis 30
3.11.4 Effect size 30
3.11.5 Linearity 31
Chapter 4 32
Results 32
4.1 SNP Quality Control Blotting Results 32
4.2 Exploratory Data Analysis 33
4.2.1 Outlier Assessment 33
4.2.2 Normality and Homogeneity of Variance 33
4.3 Neural Protein Expression 35
4.3.1 Neither social position, nor sex significantly altered GluA1 expression 35
4.3.2 Social position, but not sex, significantly altered GluA2 and GRIP1 expression. . 35
4.3.3 PICK1 and Stargazin expression were altered through a sex by position interaction. 36
4.4 Relationships between Stress, Sex, and Social Position 36
4.4.1 Stress levels significantly differed between sexes, but not social positions. 37
4.4.2 Stress levels did not strongly correlate to protein expression among any specific subgroup. 37
4.5 Effect of Linearity on Protein Expression 37
Chapter 5 39
Discussion 39
5.1 Synaptoneurosome characterization 39
5.2 Effect of social position on AMPAR subunit expression 42
5.3 Effect of social position on auxiliary AMPAR proteins 43
5.4 Stress effects on social position and neural protein expression 46
5.5 Hierarchy linearity and neural protein expression 49
Chapter 6 50
Conclusions 50
6.1 Limitations 50
6.2 Future directions and implications 52
Tables and Figures 55
References 96

List of Figures

Figure 1. AMPA receptor embedded in the post-synaptic membrane. 55
Figure 2. Tube Test schematic. 56
Figure 3. Coronal slice of a typical rat brain at the level used for the dissection (rostral view). 57
Figure 4. Synaptoneurosome protocols 58
Figure 5. Characterization of SNPs using 0.5 mL spin tubes. 59
Figure 6. Characterisation of SNPs using a 2 mL spin tube with, or without filtration. 60
Figure 7. Characterisation of SNPs using a 2 mL spin tube with pre-filtration. 61
Figure 8. Box and whisker plots using Tukey's method to identify outliers within neural protein data. 63
Figure 9. Diagnostic plots for GluA1. 64
Figure 10. Diagnostic plots for GluA2. 65
Figure 11. Diagnostic plots for GRIP1. 66
Figure 12. Diagnostic plots for PICK1. 67
Figure 13. Diagnostic plots for Stargazin. 68
Figure 14. GluA1 expression in the medial prefrontal cortex of dominant and subordinate male and female rats. 70
Figure 15. GluA2 expression in the medial prefrontal cortex of dominant and subordinate male and female rats. 72
Figure 16. GRIP1 expression in the medial prefrontal cortex of dominant and subordinate male and female rats. 74
Figure 17. PICK1 expression in the medial prefrontal cortex of dominant and subordinate male and female rats. 78
Figure 18. Stargazin expression in the medial prefrontal cortex of dominant and subordinate male and female rats. 80
Figure 19. Box and whisker plot using Tukey's method to identify outliers in corticosterone data. 81
Figure 20. Diagnostic plots for corticosterone levels. 82
Figure 21. Differences in corticosterone levels between male and female rats. 84
Figure 22. Correlation matrix of the relationship between corticosterone levels and neural protein expression among subgroup of interest. 85
Figure 23. GluA1 expression in the medial prefrontal cortex of dominant and subordinate male and female rats from stable, linear hierarchies. 91
Figure 24. GluA2 expression in the medial prefrontal cortex of dominant and subordinate male and female rats from stable, linear hierarchies. 92
Figure 25. GRIP1 expression in the medial prefrontal cortex of dominant and subordinate male and female rats from stable, linear hierarchies. 93
Figure 26. PICK1 expression in the medial prefrontal cortex of dominant and subordinate male and female rats from stable, linear hierarchies. 94

Figure 27. Stargazin expression in the medial prefrontal cortex of dominant and subordinate male and female rats from stable, linear hierarchies..... 95

List of Tables

Table 1. Summary of SNP characterisation results 62
Table 2. Summary of two-factor ANOVA test for GluA1. 69
Table 3. Summary of two-factor ANOVA test for GluA2 71
Table 4. Summary of two-factor ANOVA test for GRIP1. 73
Table 5. Summary of Tukey's HSD comparing between group differences in GluA2 expression among male and female animals. 75
Table 6. Summary of Tukey's HSD comparing between group differences in GRIP1 expression among male and female animals. 76
Table 7. Summary of two-factor ANOVA test for PICK1. 77
Table 8. Summary of two-factor ANOVA test for Stargazin. 79
Table 9. Summary of two-factor ANOVA test of corticosterone levels. 83
Table 10. Summary of one-way ANOVA test of only linear, male and female groups for GluA1. 86
Table 11. Summary of one-way ANOVA test of only linear, male and female groups for GluA2. 87
Table 12. Summary of one-way ANOVA test of only linear, male and female groups for GRIP1. 88
Table 13. Summary of one-way ANOVA test of only linear, male and female groups for PICK1. 89
Table 14. Summary of one-way ANOVA test of only linear, male and female groups for Stargazin. 90

List of Abbreviations

AMPA	α-amino-3-hydroxy-5-methyl-4-isoxazolepropionic acid
ANOVA	Analysis of Variance
ACC	Anterior cingulate cortex
BNST	Bed nucleus of the stria terminalis
co-IP	Co-immunoprecipitation
CORT	Corticosterone
CRS	Chronic restraint stress
CTD	Carboxy-terminal domain
FI	Frailty index
GRIP	Glutamate receptor interacting protein
HPA	Hypothalamic-pituitary-adrenal
HSD	Honestly significant difference
HUI	Health utility index
iGLUR	Ionotropic glutamate receptor
IQR	Interquartile range
LTD	Long-term depression
LTP	Long-term potentiation
MLRS	Mesolimbic reward system
mPFC	Medial prefrontal cortex

MWM	Morris water maze
NAcc	Nucleus accumbens
NMDA	N-methyl-D-aspartate
OTR	Oxytocin receptor
PI	Protease inhibitor cocktail
PICK	Protein interacting with C kinase
PSD	Post synaptic density
PVDF	Polyvinylidene fluoride
Q-Q	Quantile-quantile
SBN	Social behaviour network
SDMN	Social decision-making network
SDS-PAGE	Sodium dodecyl sulfate–polyacrylamide gel electrophoresis
SES	Socioeconomic status
SNP	Synaptoneurosome
SO	Sodium orthovanadate
TARP	Transmembrane AMPA receptor protein
TBST	Tris buffered saline with Tween-20
WH	Whole homogenate

Chapter 1

Introduction

1.1 Social Dominance Hierarchies

Social dominance hierarchies appear to be a universal phenomenon in social species across the animal kingdom (Strauss et al., 2022; Wang et al., 2014). Social interactions, including competition and conflict, shape dominance structures, where animals are ranked as dominant, or subordinate to one another (Sapolsky, 2005; Snyder-Mackler et al., 2020). Hierarchies in humans, non-human primates, and rodents have been extensively studied and contribute to the current knowledge of behaviors and outcomes related to an individual's rank within a hierarchy (Redhead & Power, 2022; Sapolsky, 2005; Wang et al., 2014). In pairs, or dyads of animals, dominance can be defined by agonistic interactions where one member consistently benefits, and is determined to be the dominant of the pair (Drews, 1993). Competition for resources, including access to food and mating partners, is a strong driving force influencing hierarchy formation, where dominant animals have preferential access to resources compared to their subordinates (Mooney et al., 2014).

Broadly, social hierarchies can be characterized by their linearity and steepness. A linear hierarchy is one where individual A is dominant over individual B, who is dominant over individual C, implying that individual A dominates C, this is also known as a transitive hierarchy, where animals have unique social positions (Chase et al., 2002; Varholick et al., 2019). Comparatively, in a non-linear hierarchy, one could observe a relationship where individual A dominates B, who dominates C, but then individual C is also dominant over A,

(Chase et al., 2002; Sapolsky, 2004). Hierarchy steepness is defined as the difference in winning ability between individuals in a hierarchy, where steeper hierarchies display larger differences in individual winning ability (de Vries et al., 2006). Despotic hierarchies are considered steep and linear, and typically involve one alpha and many subordinates of equivalent rank, comparatively egalitarian hierarchies are considered shallow and weakly linear with more equal resource distribution (de Vries et al., 2006; Sapolsky, 2005; Varholick et al., 2019).

Furthermore, stability of a hierarchy is a key predictor of social behaviours and outcomes, where stable hierarchies have been found to reduce conflict among conspecifics and promote survival (Tibbetts et al., 2022). Social instability is a known stressor for group-living species and has been commonly used as a stress paradigm in rodents (Beery & Kaufer, 2015; Koert et al., 2021; Strauss & Shizuka, 2022). In addition, factors such as death, natural disasters, and immigration can destabilize human hierarchies, resulting in increased competition between higher ranked individuals (Sapolsky, 2004).

The organization of social hierarchies is highly conserved among social species, and provides adaptive value to minimize conflict, divide group labour, and allocate resources (Koski et al., 2015; Tibbetts et al., 2022). Research in laboratory mice and rats, has identified differences in hierarchy phenotypes between male and female animals, where male hierarchies tend to be more linear, steep, and despotic compared to female hierarchies (Smith-Osborne et al., 2023; van den Berg et al., 2015; Williamson, Lee, et al., 2019). Sex-specific hierarchy differences are thought to be due, in part, to different social strategies employed by males and

females, where male dynamics are driven by agonistic interactions and prior experiences, whereas female dynamics are driven more by intrinsic traits (van den Berg et al., 2015). However, the current literature on female hierarchies is extremely limited, which underscores the importance of examining sex differences in social interactions and hierarchy formation.

1.1.1 Physiological Outcome of Hierarchies

In Western societies, the socioeconomic gradient of health is a strong predictor of disease outcomes and health risk behaviours, and individuals with a lower socioeconomic status (SES) will typically experience poorer health outcomes (Chen & Miller, 2013; Hertzman, 2012; Sapolsky, 2005). The first evidence supporting the social gradient of health was provided by Marmot's seminal Whitehall study, which examined social position and coronary heart disease in British civil servants. In particular, the researchers found that as an individual's occupational status level increased, their risk of coronary heart disease mortality decreased (Marmot et al., 1978). In addition, using the Health Utility Index (HUI) and the Frailty Index (FI) as health indicators, Hajizadeh et al. (2016) conducted a longitudinal analysis of socioeconomic health inequalities in Canada between 1998-2011, and found that well-educated, higher-income individuals scored higher on the HUI and lower on the FI compared to less-educated, lower-income individuals, indicating that those with a higher SES experienced better health outcomes during this time period (Hajizadeh et al., 2016). Similarly, using data from the Canadian Census Health and Environment Cohort recorded in 1996 and 2011, Bushnik et al. (2020) reported that individuals with higher levels of education, or income, had longer life and health-adjusted life expectancies.

Although SES has been used as a proxy for social position in human hierarchies, it is important to emphasize the complexity of human societies, in which a person may belong to many social networks and hierarchies at once (Redhead & Power, 2022; Sapolsky, 2005; Snyder-Mackler et al., 2020). Consequently, studies on non-human species have proven invaluable to further elucidate the effects of social status on physiological outcomes, such as reproductive success, immune function, and cardiovascular disease, where, in general, more subordinate animals experience worse outcomes (Belle et al., 2009; Bercovitch & Clarke, 1995; Chelini et al., 2011; Michopoulos et al., 2012; Sapolsky, 2004; Shively et al., 2009).

1.1.2 Social Stress

The formation of hierarchies improves social stability, reduces conflict and is a useful model to study how social rank influences an individual's stress response. The establishment and maintenance of social hierarchies can induce physical and psychosocial stress that affects both dominant and subordinate animals (Creel, 2001). However, the animal most stressed in a hierarchy is a function of the organization (e.g., despotic vs egalitarian), maintenance methods, and stability of the hierarchy, where the more stressed animal will be likely to have higher basal levels of glucocorticoids (Creel, 2001; Sapolsky, 2005). For example, in species where rank is maintained through physical reassertion on to subordinates (e.g., through aggressive behaviours), the more dominant animal is under the most stress; comparatively, subordinates are under the highest levels of stress in hierarchies where dominance is maintained through non-physical intimidation (Sapolsky, 2005). Further, clinical research involving stable hierarchies has shown that individuals with high status have reduced cortisol activity in

response to a stressor, however, when the hierarchy becomes unstable, high status seemed to increase the stress response (Knight & Mehta, 2017). In this study, undergraduate students were told they had been assigned to high or low position based on their responses to a questionnaire and were given a task. They were told their position (high or low) would either change based on their performance (unstable hierarchy) or that their performance would not influence their position (stable hierarchy). To measure stress levels, the students then completed the Trier Social Stress Test, and saliva cortisol was measured.

The most well-known part of the stress response begins with the hypothalamus being informed of a stressful stimulus, leading to activation of the hypothalamic-pituitary-adrenal (HPA) axis, which triggers glucocorticoid release from the adrenal cortex (Joëls et al., 2018). Corticosterone, the primary stress hormone in rodents, travels via the vasculature to bind its receptors, which are expressed throughout the body, and in particularly high concentrations in the hippocampus (Joëls et al., 2018). The HPA axis is a neuroendocrine system that regulates different physiological processes, and also receives negative feedback from the hippocampus (E. J. Kim et al., 2015). Notably, while acute activation of the stress response can induce adaptive changes in the brain, as the intensity and duration of a stressor increases, so does the risk for pathologies and cognitive impairment (E. J. Kim et al., 2015; McEwen, 2007).

Interestingly, previous work in mice has found that social position can affect behavioural outcomes following chronic mild stress, and that the effect plays out in a sex-specific manner (Karamihalev et al., 2020). After the application of chronic restraint stress the researchers found that subordinate status in male mice, but not female ones, was associated

with increased locomotor and exploratory behaviours seen in the open field test. Additionally, subordinate males exhibited reduced anxiety-like behaviours on the elevated plus maze, while subordinate females displayed an increase in these behaviours (Karamihalev et al., 2020). These results suggest the influence of an individual's social rank on their ability to adapt to chronic stress, and that sex-specific differences may be observed.

1.2 Neural Mechanisms of Social Interactions

When interacting with their social network, individuals must make appropriate decisions for their social context, and such social decision making involves identifying and recognizing conspecifics, learning information, and selecting an appropriate response for a situation (Gangopadhyay et al., 2021). Social decision making within a hierarchy also includes establishing position and remembering the rank of other members to appropriately express dominant, or subordinate behaviours (Lee et al., 2021). Cues commonly used to process social information include observing facial expressions in primates and olfaction in rodents (Gangopadhyay et al., 2021).

1.2.1 The Social Decision-Making Network

O'Connell & Hoffman (2011) identified the social decision-making network (SDMN) as an evolutionarily conserved network consisting of the social behaviour network (SBN) and the mesolimbic reward system (MLRS), which regulates behavioural responses to social stimuli. The SBN is comprised of the anterior hypothalamus, ventromedial hypothalamus, periaqueductal gray, and the preoptic area, while structures in the MLRS include the

basolateral amygdala, hippocampus, lateral septum, nucleus accumbens (NAcc), striatum, ventral pallidum, and the ventral tegmental area (O'Connell & Hofmann, 2011). The bed nucleus of the stria terminalis (BNST), medial amygdala, and lateral septum are involved in both networks (O'Connell & Hofmann, 2011).

Lee et al. (2021) explored how social rank influences activation of various brain regions in response to exposure to the urine of conspecifics, where urinary proteins serve as social signals. The researchers found that regions of the SDMN were differentially activated such that dominant male mice exhibited increased activation when exposed to the urine of familiar animals, while subordinates responded more robustly to the exposure of unfamiliar animals, suggesting the influence of rank on social perception (Lee et al., 2021). Further evidence for the role of the SDMN in social hierarchy is provided by Greenberg et al. (2014), who found that dominant male mice, defined as those exhibiting high levels of competitive ability, had significantly more corticotropin releasing hormone receptor 2 and estrogen receptor alpha mRNA expression in the BNST compared to subordinate mice. The researchers also found that dominant male mice had increased androgen receptor expression in the NAcc relative to subordinates (Greenberg et al., 2014). Taken together, these results provide evidence that both an animal's behaviour and the expression of mRNA and proteins in relevant neural networks can be affected by dominance hierarchies.

1.2.2 Prefrontal-Cortical Circuits

The prefrontal cortex (PFC) plays an essential role in executive functions, such as goal-directed actions, planning, decision-making, task-switching, and working memory (Fuster,

2015). In primates, the PFC is subdivided into the medial prefrontal cortex (mPFC), lateral prefrontal cortex, and the orbitofrontal cortex, where the mPFC is further divided into the infralimbic, prelimbic, and anterior cingulate cortices (ACC) (Kolk & Rakic, 2022). In rats, the PFC is divided into medial, ventral medial, lateral, and ventral regions, where the medial PFC is homologous to the dorsolateral PFC and ACC seen in primates (Kesner & Churchwell, 2011; Seamans et al., 2008). Notably, the medial PFC is involved in many important social behaviours including recognition, approach, and the inference of social status (Lee et al., 2016; Marcondes et al., 2020; Mason et al., 2014). For example, among male mice partaking in the 3-chamber test of social behaviour, increased mPFC activity was observed in response to approaching an unfamiliar mouse, but not an inanimate object or empty chamber, thus connecting mPFC activity with social approach behaviours (Lee et al., 2016). Additionally, previous studies in rodents have associated prefrontal projections to the basolateral amygdala, hypothalamus, periaqueductal grey area, and thalamus in dominance behaviours (Dulka et al., 2018; Franklin et al., 2017; Padilla-Coreano et al., 2022; Zhou et al., 2017).

Furthermore, the mPFC has been identified as a key structure influencing dominance, suggesting the need to further explore mechanisms that may explain how the region contributes to social rank (Cooper et al., 2017; Garcia-Font et al., 2022; Pallé et al., 2019; Williamson, Klein, et al., 2019; Yin et al., 2023). For example, previous work in male mice has shown after the removal of an alpha male from the hierarchy, beta males who assumed the alpha role had increased Fos activity in brain regions including the infralimbic and prelimbic cortices compared to beta males whose status did not change (Williamson, Klein, et al., 2019). The

change suggests a role for the mPFC in regulating behaviours related to social ascent within a hierarchy. Notably, Yin et al. (2023) established social position among male mice, then examined depression- and anxiety-like behaviours using various behavioural assays, and the effect of social position on activity of glutamatergic neurons in the mPFC. The researchers found significantly increased depression- and anxiety-like behaviours among subordinate males; furthermore, dominant mice had significantly increased (~60%) firing of glutamatergic neurons in the mPFC compared to subordinates (Yin et al., 2023). Taken together, these results highlight the importance of exploring molecular mechanisms underlying social rank, especially those that occur in the mPFC.

1.2.3 Neurotransmitters and Hormones

The most well studied neurotransmitter and hormone signalling systems involved in establishing and maintaining social hierarchies include the monoamines (serotonin and dopamine), as well as oxytocin, a neuropeptide. The role of serotonergic signalling in dominance behaviours, such as aggression, cooperation, and social perceptions, has been well documented (Kiser et al., 2012). Furthermore, Raleigh et al. (1991) demonstrated the influence of serotonin in mediating dominance status of male vervet monkeys. That is, pharmacological enhancement of serotonergic activity in subordinates (via tryptophan, or fluoxetine administration) was found to increase their dominance status, while reducing serotonergic function prevented the monkeys from becoming dominant (Raleigh et al., 1991). Additional evidence from Syrian hamsters, rhesus macaques, rats, naked-mole rats, and humans has also implicated serotonergic signalling in social dominance behaviours (Blanchard et al., 1991;

Janet et al., 2022; Mongillo et al., 2014; Voisin et al., 2022). For example, subordinate male rats were found to have increased levels of serotonin metabolite, 5-HIAA, in areas such as the amygdala and hippocampus compared to dominants, potentially suggesting increased serotonin metabolism in subordinates (Blanchard et al., 1991)

Similar to serotonin, dopaminergic activity has been implicated in dominance hierarchies. In dominant macaques and mice, inhibition of the D2 dopamine receptor attenuated social dominance (Yamaguchi et al., 2017). Interestingly, Morgan et al. (2002), observed an increase in D2 receptor expression in dominant, group-housed, but not socially isolated macaques, suggesting the formation of a social hierarchy lead to an increase in D2 expression (instead of the other way around). Finally, when evaluating the association between monoamine metabolite concentrations and dominance status, Kaplan et al. (2002), found increased concentrations of dopamine metabolites in the cerebrospinal fluid of dominant male and female macaques, further suggesting a role for monoamine signalling in dominance status.

Oxytocin is a key regulator of social behaviours including maternal care, social recognition, grooming, and pair-bonding (Anacker & Beery, 2013). In a stable hierarchy, dominant male rats were found to have significantly increased oxytocin receptor (OTR) binding in several brain regions, including the NAcc, compared to their subordinates (Lee et al., 2019). Additionally, Mooney et al. (2015) found increased OTR binding in the NAcc of dominant male naked mole rats compared to dominant females, suggesting potential sex-specific differences related to dominance status.

1.3 Glutamatergic Signalling

Despite advancements in the current knowledge of neural mechanisms underlying social status, there is limited literature exploring the effects of glutamatergic signalling in dominance hierarchies. As the major excitatory neurotransmitter in the mammalian brain, appropriate regulation of glutamatergic signalling is crucial, as dysfunctions have been implicated in neurodegenerative disorders, such as amyotrophic lateral sclerosis, Alzheimer's disease, and Parkinson's disease (Sheldon & Robinson, 2007). In general, glutamatergic signalling involves the synthesis of glutamate in presynaptic neurons, storage in synaptic vesicles, activity-dependent release into the synaptic cleft, and binding to receptors on the postsynaptic membrane (Sheldon & Robinson, 2007).

Ionotropic glutamate receptors (iGLURs) are ligand-gated ion channels mediating short-term changes in synaptic function, and the 3 classes of iGLURs are α-amino-3-hydroxy-5-methyl-4-isoxazolepropionic acid (AMPA), N-methyl-D-aspartate (NMDA), and kainate receptors (Hansen et al., 2021). Once released from presynaptic neurons, glutamate will bind to its post-synaptic iGLURs causing the ion channel pore to open and allowing the influx of cations that subsequently depolarize the postsynaptic cell (Hansen et al., 2021). The iGLURs are of particular interest because of their role in synaptic plasticity, including the strengthening of synaptic connections between pre- and postsynaptic neurons during long-term potentiation (LTP), and the decrease in synaptic strength resulting from long-term depression (LTD) (Bredt & Nicoll, 2003). The trafficking of the AMPA receptor (AMPAR) refers to the delivery, or removal of AMPA receptors from the postsynaptic membrane, and has been identified as a key

process regulating synaptic plasticity (Díaz-Alonso & Nicoll, 2021). In particular, the insertion of additional AMPARs in the postsynaptic membrane mediates LTP, while the endocytosis of AMPARs is involved in LTD (Bredt & Nicoll, 2003; Malinow & Malenka, 2002).

The AMPA receptors are tetrameric complexes comprised of a set of dimers combining either the GluA1, GluA2, GluA3, or GluA4 subunits, where the functional properties of the receptor differ depending on the subunit arrangement (Henley & Wilkinson, 2016; Shepherd & Huganir, 2007). For instance, GluA2-containing AMPARs are calcium impermeable, and have lower channel conductance compared to GluA2-lacking AMPARs (Isaac et al., 2007; Shepherd & Huganir, 2007). Receptors containing the GluA1/2 and GluA2/3 subunit arrangement are most prevalent, with GluA1 and GluA2 being the most broadly expressed subunits across the brain (Henley & Wilkinson, 2016). For example, using a single cell genetic approach, Lu et al. (2009) found that approximately 80% of synaptic AMPARs found at CA1 pyramidal neurons in the hippocampus were GluA1/A2 complexes, and approximately 16% were GluA2/A3 complexes.

Each AMPAR subunit is made up of an extracellular amino terminal domain which contains the ligand binding domain, a transmembrane domain, and an intracellular carboxy-terminal domain (CTD) (Díaz-Alonso & Nicoll, 2021). The CTD region across subunits is highly variable, and has been identified as a site where protein interactions and post-translational modifications such as phosphorylation occur (Henley & Wilkinson, 2016). Please see Figure 1 for a schematic of the basic structure of an AMPA receptor embedded in the postsynaptic membrane. In addition to the core AMPA receptor complex, AMPARs are

surrounded by auxiliary subunits, such as transmembrane AMPA regulatory proteins (TARPs), which are involved in the regulation of theses receptors.

1.3.1 AMPAR protein-protein interactions

The trafficking of AMPARs is highly regulated through protein-protein interactions, and is required to maintain the number of receptors expressed at the postsynaptic surface (Díaz-Alonso & Nicoll, 2021). AMPARs are found in high concentrations at the postsynaptic density (PSD), a protein-rich complex composed of cytoskeletal, regulatory, and scaffolding proteins, found in the postsynaptic membrane (Sheng & Hoogenraad, 2007). Importantly, regulation of AMPAR trafficking is mediated by protein-protein interactions between PSD proteins and the CTD region of AMPAR subunits (Bissen et al., 2019; Díaz-Alonso & Nicoll, 2021). Proteins involved in the regulation and stabilization of GluA2-containing subunits include glutamate receptor interacting proteins (GRIPs), protein interacting with C Kinase 1 (PICK1), and transmembrane AMPA regulatory proteins (TARPs) (Bissen et al., 2019).

GRIP-GluA2 interactions regulate the insertion and synaptic targeting of GluA2/3 AMPARs into the cell membrane, thus playing a role in synaptic plasticity (Bissen et al., 2019; Chung et al., 2000; Tan et al., 2020). Tan et al. (2020) demonstrated the role of GRIP1 in regulating AMPAR insertion during LTP in cultured cortical neurons, where following chemically induced LTP, there was enhancement of synaptic GluA2 and GRIP1, but not total expression of GluA subunits or GRIP1, suggesting GRIP1 is recruited to synapses during LTP. Conversely, PICK1-GluA2 interactions are implicated in the internalization of AMPARs observed during LTD (Hanley, 2008). Moreover, work in hippocampal cultures has shown that

phosphorylation and the overexpression of PICK1 decreases synaptic surface expression of GluA2 (Chung et al., 2000; Terashima et al., 2004). Interestingly, the phosphorylation of the GluA2 Serine 880 residue has been shown to decrease GluA2-GRIP1, but not GluA2-PICK1, associations in hippocampal cell culture, suggesting differential regulation of GluA2 interactions through phosphorylation (Chung et al., 2000; Matsuda et al., 1999).

In addition to GluA subunit assembly, TARPs, such as stargazin (TARP γ-2), are auxiliary proteins required for appropriate AMPAR function (Bessa-Neto & Choquet, 2023). Stargazin is known to play roles in the stabilization of AMPARs at the postsynaptic surface, that is, AMPARs do not directly bind to PSD-95, the main scaffolding protein within the PSD complex; instead, stargazin connects AMPARs and PSD-95 together (Bessa-Neto & Choquet, 2023). To illustrate the importance of the anchoring infrastructure, Bats et al. (2007) reported decreased AMPAR surface expression following the disruption of stargazin-PSD-95 interactions in cultured cells, suggesting the role of stargazin in regulating AMPAR trafficking and localization at synaptic sites. Taken together, the current evidence suggests a role for GRIPs and stargazin in the insertion and stabilization of GluA2-containing AMPARs, and a role for PICK1 in the internalization/removal of GluA2-containing AMPARs. Notably, as studies exploring AMPAR interactions with auxiliary proteins have traditionally used neuronal cell cultures, further understanding of these protein-protein interactions *in vivo* is needed.

1.3.2 AMPARs and Social Rank

In addition to the previously mentioned neural mechanisms of social dominance, recent work has implicated AMPAR function in the medial prefrontal cortex as a key mediator in the

control of social hierarchy (Park et al., 2018; Tada et al., 2016; Wang et al., 2011). Arguably, Wang et al. (2011) have provided the most convincing evidence for the role of AMPA receptors in mediating social dominance status. Using the Tube Test, the researchers established the presence of a social hierarchy among group-housed male mice and then manipulated the function of excitatory synapses in the mPFC through infection of Ras or Rap via viral recombinant DNA delivery (Wang et al., 2011). Ras and Rap are phosphatases that are known respectively to enhance and depress AMPAR trafficking to the synapse (Zhu et al., 2002). In particular, the researchers found that the dorsal mPFC exerts bidirectional control on the social rank of mice through inhibition, or promotion of AMPA receptor trafficking, where dominant mice had greater synaptic strength relative to subordinates (Wang et al., 2011). Furthermore, Park et al. (2018) explored the relationship between stress, depression, and dominance in male mice, and observed bidirectional phosphorylation of AMPARs in the mPFC of dominant and subordinates. Using both the Tube Test and chronic restraint stress (CRS) paradigm, the researchers found that CRS decreased the dominance status of the mice. Additionally, phosphorylation of the Serine 818 and 835 residues on GluA1 were highly correlated with winning points in the Tube Test (and therefore correlated with dominance status), however the phosphorylation of GluA2-Serine 880 was not (Park et al., 2018).

Although these studies implicate the role of AMPAR trafficking and expression in social dominance, only male mice were used, which limits our understanding of the mechanisms underlying dominance status in females. Interestingly, Knouse et al. (2022), observed sex-specific differences in basal glutamatergic signalling in the mPFC where female

mice exhibited higher levels of synaptosomal, but not cellular, GluA1 and GluA2 subunit expression, suggesting female mice have increased synaptic expression of AMPARs compared to males. Additionally the researchers observed increased amplitude and frequency of excitatory postsynaptic currents in female mice suggesting females have enhanced glutamatergic transmission in the mPFC (Knouse et al., 2022). Taken together, these results support the need to explore sex-specific mechanisms underlying dominance.

Chapter 2

Specific Aims

2.1 Rationale

The identification of the medial PFC as a driver of social dominance status and related social behaviours has led to increased interest in AMPAR-mediated mechanisms that might underlie social rank, however, there is a clear paucity of research exploring the details of AMPAR activity implicated in dominance. Despite recent advancements in our knowledge of how AMPARs may influence dominance status, to date, no studies have explored AMPAR auxiliary proteins in the context of social rank. Furthermore, no studies have explored AMPARs, or their auxiliary proteins in the medial PFC of female animals; therefore, the current understanding of the cellular mechanisms underlying the role played by the mPFC in female social dynamics is extremely limited. As a result of the points raised, the proposed research aimed to elucidate the activity of key AMPAR subunits, and their primary auxiliary proteins, with social rank in both male and female rats.

2.2 Study Objectives

The proposed research questions are as follows:

1. How does social position affect the expression of the GluA1 and GluA2 AMPA receptor subunits and their associated auxiliary proteins in the medial prefrontal cortex?
2. Are there sex-specific differences in the expression of these proteins?

3. Could differences in perceived stress influenced by social position affect the expression of these proteins in the medial prefrontal cortex?
4. Does hierarchy linearity influence the relationship between social position and neural protein expression?

2.3 Hypotheses

Based on the current literature, the hypothesized results are as follows:

1. Higher ranked animals will have increased expression of GluA1, GluA2, GRIP1, and stargazin, and decreased expression of PICK1, compared to their subordinates.
2. Female animals will exhibit increased AMPAR subunit expression compared to males.
3. Animals with higher levels of stress will exhibit lower levels of AMPAR subunit expression, and this association will differ between males and females.
4. In linear hierarchies we will observe a greater level of difference in neural protein expression between dominant and subordinate animals.

Chapter 3

Methods

3.1 Animals

Adult, 14-week-old, male and female Sprague-Dawley rats were group-housed by sex in sets of four (n = 10 groups) for two weeks prior to behavioural testing. The animals were housed on a 12-hour reverse light cycle (with lights off at 8 am), at a constant temperature (approximately 21°C), with ad libitum access to standard rodent chow (Teklad 22/5, Envigo) and water. Behavioral experiments were approved by University of Waterloo Animal Care Committee (ORE 44254).

3.2 Behavioural Experiments

The Tube Test was used to determine the social position of the group-housed rats. The Tube Test apparatus was composed of two holding chambers (length 20 cm, width 20 cm, height 15 cm) connected by a plexiglass tube (length 100 cm, diameter 7.0 cm). The holding chambers were separated from the tube with a sliding door; as well, a sliding door was present in the middle of the tube. Please see Figure 2 for a schematic of the Tube Test paradigm. Prior to the test, each group was habituated to the apparatus for 2 days. Habituation involved the transfer of a group of rats from the housing room to the testing room where they were left for 15 minutes in individual cages. After the 15 minutes of acclimatization, each rat was handled one at a time for 5 minutes, and then placed in a holding chamber and allowed to explore the

Tube Test apparatus. Once the rat had moved back-and-forth across the tube 10x, it was returned to its cage and the apparatus was cleaned with 70% ethanol before the next rat was allowed to explore the apparatus. Following habituation, group-housed rats underwent the Tube Test paradigm for 3 days. All 4 group-housed rats were tested against one another in the Tube Test, for a total of 6 pairs, where each pair was tested twice by starting in alternating holding chambers, resulting in 12 total matches per group.

To begin a trial, all three sliding doors were shut, and a rat was placed in each holding cage. The doors separating the chambers from the tube were opened, allowing the rats to walk to the middle of the tube; at this time, the central sliding door would be opened, which ensured both rats started the trial in the middle of the tube. The winner of the trial was the rat that pushed the other back into its starting chamber, and would receive 1 point, while the losing rat did not receive any points. After the last trial of the day the rats were returned to their group cages. The number of points for each rat was calculated using David's Score, resulting in a rank from 1-4, where animals ranked as 1 (alpha animals) were the most dominant, and those ranked at 4 (delta animals) were the least dominant. The ranks from these dominance scores were used for the immunoblotting analysis.

Following day 3 of the Tube Test, the Morris water maze (MWM) was performed to assess spatial learning and memory. The main components of the MWM are spatial acquisition (4 days), probe test (1 day), and spatial reversal (2 days), MWM testing followed the protocol previously described by Davari et al. (2023). After the last day of MWM testing, one final tube test was conducted to test the stability of the hierarchy over the 1-week period.

3.3 Blood and Brain Tissue Collection

One day after the last Tube Test, the animals underwent anesthesia in a chamber with >60% carbon dioxide, and were then decapitated. Trunk blood was collected and allowed to clot for 20 minutes at room temperature and then centrifuged (1,800 x g for 20 minutes). The supernatant (that is, serum) was flash-frozen in liquid nitrogen and stored at -80ºC before being sent for analysis at the Drug Safety Laboratory at Western University using a previously described procedure (Gow et al., 2011). Each brain was quickly extracted and placed in a rat brain mold (Ted Pella, Inc.) submerged in artificial cerebrospinal fluid (composed of 124 mM NaCl, 26 mM $NaHCO_3$, 3 mM KCl, 2 mM $CaCl_2$, 1.2 mM NaH_2PO_4, 10 mM glucose, 10 mM HEPES, and adjusted to pH 7.37-7.43). A coronal slice of tissue from the frontal region (between the 5^{th} and 8^{th} slots of the brain mold) was taken, from which the mPFC was dissected, snap-frozen in liquid nitrogen, and stored at -80ºC. Please see Figure 3 for a coronal tissue slice indicating the region where the medial PFC was dissected.

3.4 Synaptoneurosome Preparation

Synaptoneurosomes (SNPs) are enrichments of pre- and post-synaptic terminals, and are usually prepared by sequentially passing homogenates through syringe-driven filters of decreasing pore size (Villasana et al., 2006). During this process inter-experimenter variability can arise due to differences in the manual application of pressure to the syringe-driven filters, leading to a shift towards centrifuge-driven filters (Murphy et al., 2014); however, it was unclear whether this method would work well with our tissue samples. As a result, three

protocols were examined in an attempt to achieve consistent synaptic enrichment of mPFC samples: two-step syringe filtration, spin-tube filtration, and syringe-driven filtration followed by spin-tube filtration (each of these will be discussed below).

3.4.1 Two-step syringe-driven filtration

Our laboratory has previously used a two-step syringe-driven method to prepare SNPs from hippocampal samples (Figure 4A) however as we had never used this procedure with medial PFC tissue, we first aimed to characterize the SNP preparation technique with mPFC to ensure synaptic enrichment was possible prior to beginning work on the study samples.

Frozen mPFC tissue was placed in a 2 mL glass homogenizing tube, over ice, and homogenized using 30-40 manual strokes with a total of 1 mL of 1X modified Krebs buffer, which was composed of 118.50 mM NaCl, 4.70 mM KCl, 2.50 mM $CaCl_2 \cdot 2H_2O$, 1.18 mM $MgCl_2 \cdot 6H_2O$, 1.18 mM KH_2PO_4, 24.90 mM $NaHCO_3$, 10.00 mM glucose (pH 7.40), and supplemented with the P8340 protease inhibitor cocktail (PI) and sodium orthovanadate (SO). Samples were then decanted into a 1.5 mL Eppendorf tube, and allowed to sit for 10 minutes to allow for gravity sedimentation of nuclear material.

Prior to filtering the remaining homogenate sample, the filter holders were assembled. The homogenate was first filtered through three 100 µm Millipore nylon net filters held in a 25-mm stainless-steel Millipore syringe filter unit, which were pre-wet with 1X Krebs buffer. The filtrate was collected in an Eppendorf tube and then subsequently filtered through one 5 µm Millipore nitrocellulose net filter held in a 13-mm stainless steel Millipore syringe filter holder. The resulting filtrate was centrifuged at 1000 x g, for 15 min at 4°C. The supernatant

(cytosolic fraction) was discarded, and the pellet (synaptoneurosome fraction) was resuspended using 200 µL of non-ionizing lysis buffer [composed of 100 mM NaCl, 25 mM EDTA, 10 mM Tris solution, 1% (v/v) Triton X-100, 1% (v/v) IGEPAL CA-630] with PI and SO added, and stored at -80°C.

3.4.2 Spin-tube filtration

Due to concerns around inter-experimental variability with the two-step method, further modifications to the SNP protocol were undertaken. To increase synaptic enrichment and throughput we attempted to use the spin-tube filtration method to enrich synaptoneurosomes (Figure 4B). In this protocol, each frozen mPFC was placed in a 2 mL glass homogenizing tube and homogenized using 30-40 manual strokes over ice, with a total of 1 mL of 1X modified Krebs buffer. For blotting a 100 µL aliquot of the supernatant was collected as the whole homogenate (WH) sample. To allow for gravity sedimentation, the homogenate was decanted into a 1.5 mL Eppendorf tube and kept on ice for 10 minutes. The homogenate was then equally decanted into the upper chamber of either one, or two 0.5 mL Ultrafree-MC Centrifugal Filter spin tubes (5 µm pore size), and 50 µL of 1X Krebs buffer was added to yield a total volume of 500 µL. The tubes were then centrifuged at 15,000 x g for 5 min at 4°C. The upper chambers were discarded, and the pellet in each lower chamber was resuspended in 100 µL of 1X non-ionizing lysis buffer, then combined into a 1.5 mL Eppendorf tube.

As the 0.5 mL tubes did not provide adequate enrichment of synaptic proteins, we moved towards using 2 mL spin tubes as their larger size would potentially provide a greater

surface area to filter the tissue. The protocol for the 2 mL spin tube method was the same as the 0.5 mL tubes, however the spin speed and temperature varied (3,200 x g vs 3,500 x g, 4°C vs room temperature).

3.4.3 Syringe-driven filtration followed by spin-tube filtration.

The final protocol modification to the SNP process was to include a pre-filtration step prior to using the 2 mL spin tube (Figure 4C). To test if the enrichment would vary across brain regions, we used both mPFC and septal hippocampus samples with this protocol. Similar to Sections 3.4.1 and 3.4.2, frozen tissue was homogenized in a 2 ml glass tube with 1X Krebs buffer, gravity sedimentation was performed, and an aliquot of the whole homogenate sample was collected. The tissue sample was then pre-filtered through three pre-wet Millipore nylon net filters (100 µm pore size) in a 25-mm stainless steel Millipore syringe filter holder. The filtrate was collected directly into the upper chamber of the 2 mL spin tube to which 1X Krebs buffer (with PI and SO) was added to bring the solution to 1.5 mL in order to dilute the sample. The spin tubes were initially spun at 3,200 x g for 15 min at 4°C. The spin speed, time, and temperature were manipulated to determine the most optimal conditions. The content in the upper chamber and the supernatant of the lower chamber were discarded, and the pellet was resuspended in 1X non-ionizing lysis buffer and then stored at -80°C.

3.5 Protein Assay

Protein concentrations of all the samples were determined using a BioRad DC Protein Assay kit according to the manufacturer's guidelines, where bovine serum albumin was used to create a standard curve of known concentrations. The BioTek PowerWaveX 340 spectrophotometer was used to read the sample absorbance values at 750 nm.

3.6 Quality Control Blotting of SNPs

To determine whether the various SNP protocol modifications enriched synaptic proteins, quality control immunoblotting of the samples using a PSD-95 antibody was undertaken. Since PSD-95 is abundantly expressed at the post-synapse, and is often used as a marker of the postsynaptic density (Villasana et al., 2006), we expected to observe the protein in greater abundance in the SNPs than in whole homogenates.

3.7 Preparation of Medial Prefrontal Cortex Homogenates

Due to the inconsistent synaptic enrichment of mPFC tissue (Section 3.4), the decision was made to examine whole homogenate samples. To prepare whole tissue homogenates, frozen mPFC samples were placed into a 2 mL glass homogenizing tube to which 2 mL of 1X non-ionizing lysis buffer was added. Manual homogenization using 20 strokes over ice was performed. The homogenate was equally decanted into two 1.5 mL tubes and centrifuged at 1000 x g for 10 min at 4^{o}C. The supernatant from each tube (that is, the post-nuclear fraction) was combined, vortexed, and aliquoted, after which a protein assay was conducted before the samples were stored at -80°C.

3.8 Standard Curve Optimization

To determine the optimal loading concentrations of mPFC homogenates, optimization blots using the primary antibodies of interest were constructed (following steps described in the subsequent section). For each blot, 5, 10, 15, and 20 µg of mPFC tissue was loaded in duplicate, and immunoblotting was done using antibodies for GluA1, GluA2, GRIP1, PICK1, and stargazin. Overall, loading 15 µg of sample in each lane was determined to provide the most clear, unsaturated signal for all 5 proteins. We also performed a secondary antibody control test to assess for holdover effects and non-specific binding, as the membranes would be sequentially stripped and reprobed during the blotting process.

3.9 SDS-PAGE and Western blotting

Western blotting was used to determine the effects of social position on the expression of GluA1, GluA2, GRIP1, PICK1, and stargazin in the medial prefrontal cortex of male and female rats. On the day of electrophoresis, the mPFC tissue samples were removed from the -80ºC freezer and left to thaw on ice. Equal volumes of tissue and sample buffer were combined, vortexed (1-2 s), centrifuged (1000 x g, 20 s, 4°C), and then heated at 95°C (5 min). For each group, 15 µg of protein samples (in duplicate), and a reference sample of whole PFC (collected from an adult, male, Sprague-Dawley rat that was not a part of the current study) were loaded into 10-well, 10% polyacrylamide gels in the following order: male-alpha, male-delta, female-alpha, female-delta, duplicate samples, and reference sample. The gels were run at 200 V for approximately 1 h and were then soaked for 15 min in chilled transfer buffer [composed of 25

mM Tris, 192 mM glycine, and 10% (v/v) methanol]. Proteins were then transferred from the gel to a pre-treated PVDF membrane at 90 V for 2 h at 4°C. After transfer, the blots were incubated with Ponceau S for 10 min, washed with T1 water, left to air dry, and then imaged using SNAPGENE software.

Each membrane was cut at approximately 75 kDa to allow concurrent immunoblotting of proteins at different molecular weights. All membranes were blocked for 1 h in Tris-buffered saline with Tween-20 (TBST) [composed of 20 mM Tris, 138 mM NaCl, 0.1% Tween-20 (v/v), at pH 7.6] using 5% (w/v) bovine serum albumin, except when probing for stargazin where membranes were blocked using 3% (w/v) skim milk. After blocking, membranes were incubated at 4°C overnight with the appropriate primary antibody prepared in blocking buffer (1:1000). The primary antibodies used were anti-GluA1 rabbit monoclonal (Cell Signaling Cat #13185S), anti-GluA2 rabbit monoclonal (Cell Signaling Cat #13607), anti-GRIP1 mouse monoclonal (Santa Cruz Biotechnology sc-365937), anti-PICK1 rabbit monoclonal (Abcam ab3420), and anti-stargazin rabbit monoclonal (Millipore Sigma, AB9876). After the primary antibody incubation ended, the membranes were washed 3 x 10 min with TBST. Next, each membrane was incubated with either a mouse (Santa Cruz Biotechnology sc-516102), or rabbit (Santa Cruz Biotechnology sc-2357) secondary antibody prepared in blocking buffer (1:5000) for 1 h at room temperature, washed with TBST for 3 x 10 min, treated with Crescendo for 5 min, and imaged.

3.10 Immunoblotting Data Analysis

Densitometric analysis of membranes was performed using the NIH Image J software. Optical density data from Image J were compiled in Microsoft Excel, and analysis was conducted in GraphPad Prism and R Studio. To determine the effect of social position on the expression of our proteins of interest, optical densities of each relevant band in each blot were measured and normalized to the optical density of their respective Ponceau S stain value (to control for loading variation). The normalized duplicate values were then averaged and expressed as a percentage of the reference sample band for the same blot (to control for inter-blot variation). For example, the Group 1 alpha-male, delta-male, alpha-female, and delta-female values were expressed as a percentage of the reference sample band from their specific blot.

3.11 Statistical Analysis

3.11.1 Testing assumptions of parametric tests

Prior to running our main analyses we used box and whisker plots to assess for potential outliers. The plots were created using Tukey's method where the 'box' is the interquartile range (IQR), which is the difference between the 25^{th} (Q1) and 75^{th} (Q3) percentiles. The lower whisker was calculated by subtracting 1.5 x IQR from Q1, and the upper whisker was calculated by adding 1.5 x IQR to Q3. Outliers were determined as points outside of the whiskers. Tukey's method was used to identify outliers as it provides insight into the

distribution of the data and, unlike other methods of outlier detection (such as Grubbs test), does not rely on the data being normally distributed.

To determine the appropriateness of an ANOVA model, we first assessed the data to confirm whether they fit the assumptions for parametric tests, that is, independence of observations, normality, and homogeneity of variance. Each of the samples used in this study came from a different rat, ensuring independence of each tissue sample. To assess whether the data followed a normal distribution both graphical (quantile-quantile [Q-Q] plot) and quantitative (Shapiro-Wilk test) assessments were used. The Shapiro-Wilk test was chosen as it is appropriate for small sample sizes (Mishra et al., 2019). Normally distributed data typically show a diagonal, approximately linear scatter on a Q-Q plot, and a non-significant result on the Shapiro-Wilk test ($p > .05$). Homogeneity of variance was assessed graphically (residual versus fitted values) and statistically (Levene's test), where a statistically non-significant result ($p > .05$) indicates the groups have equal variances.

3.11.2 Immunoblotting data – Two-factor ANOVA design

To examine the effects of sex and social position on our proteins of interest (GluA1, GluA2, GRIP1, PICK1, and stargazin) we used a 2-factor ANOVA model (factor 1 = sex, factor 2 = social position) where animal group (also known as batch) was considered a blocking variable. A blocking variable is considered a nuisance variable as it introduces variation that can conceal the actual effect of interest (Gaskill & Garner, 2020). The inclusion of group as a blocking variable in the ANOVA model allows us to account for potential variation caused by the animals being ordered and examined at different times. That is, the animals were received

from the vendor in different "batches", which means that they may have had different transportation and husbandry-related experiences. When a statistically significant omnibus p value (< .05) was observed, such that at least one of the group means was different from the others, Tukey's Honestly significant difference (HSD) test was used as the post-hoc test to further examine differences among groups. Tukey's HSD is a pair-wise post-hoc test that tests every possible pairing and controls for the family-wise error rate, which is the probability of observing a false positive (Type 1 error) (H.-Y. Kim, 2015).

3.11.3 Immunoblotting data – Corticosterone Analysis

We used a 2-factor ANOVA with corticosterone level as the outcome, sex and position as the main effects, and group as a blocking variable, to explore if there was an interaction between these variables (that is, whether the effect of sex on CORT levels depended on position, or vice versa). Further, to understand the relationship between stress and neural protein expression on our subgroups of interest (alpha-male, delta-male, alpha-female, delta-female) we ran a correlational analysis using the Pearson correlation coefficient (r).

3.11.4 Effect size

To complement the statistically significant ANOVA results, we elected to examine their practical significance using the eta-squared (η^2) effect size measure. Eta-squared is a measure of association that represents the proportion of variance in the dependent variable (neural protein expression) explained by our independent variables (sex and position) (Richardson, 2011). We applied the eta-squared conventions of small ($\eta^2 = 0.01$), moderate

(η^2 = 0.06), and large (η^2 = 0.14). When examining the effect sizes of the post-hoc results we used Cohen's d, which represents the standardized mean difference between two groups (Lakens, 2013). The standard conventions of small (d = 0.2), medium (d = 0.5), and large (d = 0.8) were used.

3.11.5 Linearity

Finally, we were interested in the potential effect of hierarchy linearity on neural protein expression; that is, whether we would observe greater differences between alpha and delta animals in linear hierarchies compared to non-linear ones. As noted in Section 3.2, the linearity structure of the male and female groups was measured twice, once after the initial 3 days of the Tube Test and then again 1 week later (before euthanasia), and a stable, linear hierarchy was defined as a group that had a linear structure at both time points. Of the 10 groups that were measured, only 4 male groups and 3 female groups were found to have a linear structure at both time points. Due to the modest sample size, we ran a one-factor ANOVA for this exploratory analysis, with position as the main effect, group as a blocking variable, and male and female hierarchies considered separately.

Chapter 4

Results

4.1 SNP Quality Control Blotting Results

Although the syringe driven, two-step filtration method was initially considered to prepare SNPs, concerns over inter-experimental variability motivated the switch to alternative SNP preparation approaches. Overall, to assess whether the spin-tube method or pre-filtration protocols enriched synaptic proteins, immunoblotting was performed on mPFC and hippocampal samples using a PSD-95 antibody. Some level of enrichment was found in 9/19 samples; however, results were inconsistent when using the same protocol conditions on different mPFC samples (Table 1).

Notably, the spin tube method using 0.5 mL spin tubes did not show greater PSD-95 expression in SNPs relative to WH sample (Figure 5). Observation of the spin tubes after centrifugation showed a considerable amount of tissue within the upper chamber that had not passed through, suggesting the surface area was too little for the volume of tissue loaded such that synaptic proteins were getting stuck in the upper chamber. To address this concern we moved to using 2 mL spin tubes either with, or without pre-filtration using the 100 µm 25-mm filter unit. The highest, most consistent degree of enrichment was found when homogenates were pre-filtered with a 100 µm syringe-driven filter and then placed in a centrifuge-driven filter that was spun at 3,200 x g for 15 minutes at room temperature. Interestingly, when preparing synaptoneurosomes with these conditions both high (Figure 6) and minimal Figure

7) levels of enrichment were observed in mPFC tissue, suggesting inter-experimental variability leading to these differing results.

Despite our preliminary results showing that the centrifuge-driven filtration method can successfully prepare synaptoneurosomes, further refinements are needed to determine the optimal conditions. Given concerns regarding variability across preparations that arose when optimizing the SNP protocols, we elected to use whole homogenate preparations when examining the study samples.

4.2 Exploratory Data Analysis

4.2.1 Outlier Assessment

Box and whisker plots, stratified by sex, were created using Tukey's method to identify potential outliers (Figure 8). Two outliers were identified, one from the female GluA1 group, and one from the male stargazin group. Notably, both GluA1 and stargazin were normally distributed based on graphical and statistical measures (Section 4.2.2). As the outliers did not affect the data distribution, and considering our relatively small sample size, we elected to keep these points in our dataset.

4.2.2 Normality and Homogeneity of Variance

Normality of the data was assessed using the Shapiro-Wilk test and Q-Q plots, where the null hypothesis for the Shapiro-Wilk test was that the data are normally distributed and the alternative hypothesis was that the data did not come from a normal distribution. When

assessing Q-Q plots, the data were considered normally distributed if the points were arranged in relatively close proximity to a positive, diagonal line.

The results of the Shapiro-Wilk test for GluA1, GRIP1, PICK1, and stargazin were not statistically significant ($p > .05$), indicating that these data are normally distributed. The Shapiro-Wilk test for GluA2, however, resulted in a rejection of the null hypothesis ($p = 0.0018$). The Q-Q plots of the residuals for all datasets revealed approximately linear, diagonal lines for each protein of interest (Figure 9-Figure 13). Upon examination of the Q-Q plot for GluA2 (Figure 10), there appeared to be one data point skewing the distribution. When the data point was removed, GluA2 was able to pass the Shapiro-Wilk test ($p > .05$), however, due to our modest sample size, we elected to keep this point in the dataset.

Homogeneity of variance was assessed using both Levene's test and examination of a plot of residual versus fitted values. The null hypothesis of Levene's test is that the data variances are equal. When assessing the residual plots, we would expect to see no apparent pattern across the 0 line if variances are equal. The results of Levene's test were not statistically significant for any of the data sets ($p > .05$), and there was no apparent pattern observed in the residual versus fitted plots (Figure 9-Figure 13). Taken together, the results of both the graphical and statistical testing suggest the data fit the assumptions underlying parametric tests, and a two-factor ANOVA would be appropriate to use when analyzing the immunoblot data.

4.3 Neural Protein Expression

4.3.1 Neither social position, nor sex significantly altered GluA1 expression

We did not observe a significant effect of position [$F(1, 27) = 2.35$, $p = .137$], sex [$F(1, 27) = 0.48$, $p = .494$], or their interaction [$F(1, 27) = 2.98$, $p = .096$] on GluA1 expression (Table 2, Figure 14). In addition, there was only a small-moderate effect size of position ($\eta^2 = .029$) and the sex by position interaction ($\eta^2 = .036$).

4.3.2 Social position, but not sex, significantly altered GluA2 and GRIP1 expression.

Our ANOVA analysis showed position-specific differences in GluA2 [$F(1, 27) = 4.23$, $p = .049$] (Table 3, Figure 15) and GRIP1 expression [$F(1, 27) = 7.18$, $p = .012$] (Table 4, Figure 16). In contrast, a statistically significant influence of sex was not found on either GluA2 expression [$F(1, 27) = 0.22$, $p = .644$], or GRIP1 expression [$F(1, 27) = 3.42$, $p = .076$]. Notably, moderate effect sizes were observed for position on both GluA2 ($\eta^2 = .081$) and GRIP1 ($\eta^2 = .095$) expression.

Tukey's HSD was used as the post-hoc test to compare differences between group means. To reduce the risk of increasing the family-wise error rate that can be caused by completing multiple comparisons, and because sex was not a significant factor, we chose to look within the sexes when considering specific group differences, and only examined alpha- and delta-males and alpha- and delta-females. Neither the difference in GluA2 expression between alpha- and delta-males, nor alpha- and delta-females was statistically significant ($p > .05$) (Table 5). Comparatively, the difference in GRIP1 expression between alpha- and delta-

males was statistically significant ($p = .048$), with a large Cohen's d value ($d = 0.802$) (Table 6).

4.3.3 PICK1 and Stargazin expression were altered through a sex by position interaction.

We observed a significant interaction of our main effects, sex and position, for both PICK1 [$F(1, 27) = 4.33$, $p = .047$] (Table 7, Figure 17), and stargazin [$F(1, 27) = 4.64$, $p = .040$] (Table 8, Figure 18). However, the effect sizes of the interaction effects for PICK1 ($\eta^2 = .011$) and stargazin ($\eta^2 = .012$) were small. Notably, although there was a significant main effect of sex on PICK1 expression, and a significant main effect of position on stargazin expression, the presence of an interaction effect makes interpreting the main effects difficult, therefore we will only discuss the interaction effect.

4.4 Relationships between Stress, Sex, and Social Position

To explore if the stress levels of the animals differed based on sex, social position, or their interaction, we ran a 2-factor ANOVA with corticosterone (CORT) values as our outcome. We first assessed the corticosterone data for assumptions of parametric tests, which uncovered two outliers among the alpha and delta female groups (Figure 19). The data set did not pass the Shapiro-Wilk test for normality ($p < .05$), and had a slightly curved line on the Q-Q plot, however it did pass Levene's test. After removal of the two noted data points the data were normally distributed and fit the assumptions of parametric tests (Figure 20). We chose to remove the two outliers in this case as they were affecting the distribution of the data.

4.4.1 Stress levels significantly differed between sexes, but not social positions.

We found that CORT levels significantly differed between the sexes [$F(1, 25) = 12.68$, $p = .002$], but not between social positions [$F(1, 25) = 0.60$, $p = .445$] (Table 9). Additionally, the interaction between sex and social position on CORT levels was non-significant [$F(1, 25) = 2.11$, $p = .158$]. A strong effect size for sex was observed ($\eta^2 = 0.287$). Female rats were found to have approximately double the level of corticosterone compared to male rats (Figure 21).

4.4.2 Stress levels did not strongly correlate to protein expression among any specific subgroup.

To assess whether the stress levels of the animals were related to neural protein expression, we ran a correlation analysis on our subgroups of interest (alpha-males, delta-males, alpha-females, and delta-females). When examining the strongest relationships across the subgroups, stargazin and CORT were moderately, negatively correlated among alpha-males ($r = -0.55$); comparatively, delta-males showed a weak, positive relationship between GluA1 and CORT ($r = 0.36$). Conversely, the GRIP1-CORT relationship was moderately, positive in both alpha ($r = 0.43$) and delta ($r = 0.58$) females (Figure 22).

4.5 Effect of Linearity on Protein Expression

Finally, to explore the potential influence of hierarchy linearity, we ran a one-factor ANOVA with social position as the main effect on the stable linear, male and female groups separately. We chose to only include groups that were linear throughout the behavioural

experiments (that is, during both the initial test and at re-test a week later), and only 4 male (40% of the total) and 3 female (30% of the total) hierarchies fit this criterion.

Among male animals, position did not appear to have a significant effect upon any of the proteins of interest. Among female animals, however, the position effect for stargazin was significant, with a considerably large Cohen's d [$F(1, 2) = 41.46$, $p = .023$, $d = 2.02$] (Table 10-Table 14, Figure 23-Figure 27).

Chapter 5

Discussion

5.1 Synaptoneurosome characterization

Glutamate plays a significant role in neuronal functions such as synaptic plasticity, but also in pathophysiologies related to excitotoxicity (Malinow & Malenka, 2002; Sheldon & Robinson, 2007). Consequently, studying glutamatergic synapses is of great importance. For several decades, synaptoneurosome preparations have been a common technique to isolate glutamatergic synapses. Synaptoneurosomes are defined as structures containing resealed pre- and post-synaptic sacs and are typically prepared through serial filtration (Hollingsworth et al., 1985).

We attempted to develop a method to prepare synaptoneurosomes from the medial prefrontal cortex of adult rats. Our goal was to standardize the SNP method to achieve consistent synaptic enrichment by removing the inter-experimenter variability that can arise from the traditional method that uses syringe-driven filtration. During the characterization process the main variables we chose to manipulate were spin tube volume (0.5 vs 2 mL), spin speed (3,200 vs 3,500 x g), and temperature of the centrifuge (4°C vs room temperature). By examining a combination of syringe- and centrifuge- driven methods, we found the most consistent degree of enrichment when first pre-filtering the tissue samples using a 100 μm syringe-driven filter, then centrifuging the filtrate at 3,200 x g for 15 minutes at room temperature.

Of the 19 samples used to characterize the method, 9 achieved some level (low, moderate, or high) of synaptic enrichment (defined as greater PSD-95 levels in SNPs compared to whole homogenates). Two of these samples achieved moderate (1.4-1.5x) enrichment and 3 samples achieved high (>2x) levels of synaptic enrichment. Our results are consistent with previously published work by Murphy et al. (2014) who used tissue from the somatosensory cortex of adult rats, and frontal cortex of cats when comparing filter-driven synaptoneurosome preparations to a centrifuge-driven, high-throughput method. In their protocol, the syringe-driven, SNPs were manually homogenized and then pushed through a 5 µm filter holder, while the centrifuge-driven samples were homogenized in an automatic homogenizer and then transferred to a 5 µm centrifugal filter unit (spin tube) before being centrifuged at 12,000 x g for up to 4 minutes and then again at 1000 x g for 20 minutes. Centrifugation was done in cooled centrifuges. The researchers found, on average, a 1.6x greater synaptic enrichment of PSD-95 in the manually prepared synaptoneurosomes compared to whole homogenate, whereas the high-throughput method achieved, on average, a 2.7x greater synaptic enrichment compared to whole homogenates (Murphy et al., 2014).

One observation we found when characterizing the SNP protocol was the inconsistency in PSD-95 enrichment even when using the same conditions, suggesting inter-experimental variability leading to differing results. Potential sources of variation across the synaptoneurosome preparation method are the homogenization and syringe-driven filtration steps, which are done manually and can differ by the number of homogenization strokes, method of homogenization (that is, whether the pestle is twisted as it moves up and down inside

the homogenizing tube), and the amount of pressure used to push the homogenate through the filter unit. While an automated, high-throughput SNP preparation could reduce these sources of variation, our results have shown that a combination of syringe- and centrifuge-driven techniques can achieve high levels of PSD-95 enrichment in synaptoneurosomes, and future experiments should work to standardize these manual steps as much as possible.

Furthermore, when reviewing our immunoblotting data for potential sources of variation, we noticed some differences in the Ponceau S staining between whole homogenate and synaptoneurosome samples, even though the same amount of WH and SNP protein was loaded. Ponceau S is a total protein stain that binds to positively changed amino acid groups, and is typically used to control for variability in the amount of protein loaded on a blot (Sander et al., 2019; Thacker et al., 2016). Qualitatively, we found greater Ponceau S staining of whole homogenate samples compared to SNPs on the same blot, suggesting there were decreased levels of basic proteins in SNP preparations compared to whole homogenates. Our observations strongly suggest that the SNP process is changing the protein composition of the whole homogenate. To understand what the enrichment process may be doing, an important next step would be to probe for proteins that should be more abundant in whole brain homogenates, such as glial fibrillary acidic protein (GFAP), which is an astrocyte marker, and Golgi proteins, which are non-synaptic cellular markers. We would expect the expression of these non-synaptic proteins to be greater in homogenates compared to synaptoneurosomes. These data, in addition to measurement of PSD-95 levels, would provide information on how the SNP process is changing the whole homogenate.

5.2 Effect of social position on AMPAR subunit expression

Interactions between conspecifics form the basis for hierarchy formation in social species (Strauss et al., 2022). Manipulation of AMPA receptor function has been found to alter social behaviours, leading to our interest in studying the GluA1 and GluA2 subunits in the context of social rank (Park et al., 2018; Wang et al., 2011). To examine the effects of social position, sex, and their interaction on GluA subunit expression we used a 2-way ANOVA model when analyzing the immunoblotting data we had collected. We hypothesized that dominant animals would have greater GluA1 and GluA2 expression compared to subordinates, and that this relationship would be more apparent in female rats compared to male rats.

We did not find evidence that either social position, or sex affected GluA1 expression in the medial prefrontal cortex. However, we did find evidence for the role of social position on GluA2 expression. Since we did not find evidence of a main effect of sex, or an interaction between social position and sex, we concluded that social position influences GluA2 expression independent of sex. Though not statistically significant, GluA2-expression was found to be greater in alpha-males (~18%) and alpha-females (~10%) compared to their subordinates.

Our GluA2 results align with the current literature on male rodents, where dominant male mice exhibited increased excitatory synaptic strength in the dorsal mPFC compared to their subordinates, suggesting these mice have increased AMPAR expression (Wang et al., 2011). Although the magnitude of difference between alpha- and delta- males in our study was not statistically significant, the direction of difference (increased expression in alpha-males),

follows what is seen in the literature. There are no current studies that we know of that have explored AMPAR expression in female rat hierarchies, to be able to compare our results to.

An additional aim of this study was to examine sex-specific differences in the expression of GluA subunits. Notably, we did not find evidence of differences in either GluA1, or GluA2 expression between adult male and female rats. In contrast, previous work has found increased glutamatergic transmission and approximately double the amount of basal levels of synaptosomal, but not total, expression of GluA1 and GluA2 subunits in the medial PFC of female rats compared to male rats (Knouse et al., 2022). The differences in GluA expression seen in synaptosomal versus whole tissue suggests a potential reason for the lack of sex-differences observed in this study, is due to the use of mPFC homogenates, and not synaptic enrichments.

5.3 Effect of social position on auxiliary AMPAR proteins

In addition to examining expression of the GluA1 and GluA2 subunits, we also explored how social rank influences expression of the AMPAR auxiliary proteins (GRIP1, PICK1, and stargazin). To the best of our knowledge, no previous studies have explored the effect of social position on levels of the auxiliary proteins, which removed our ability to have a sense as to what could be expected. However, since we hypothesized dominant animals would have increased AMPAR expression compared to their subordinates, we also expected dominant animals would have increased GRIP1 expression due to its role in AMPAR insertion at the synapse. Our analyses found that social position, but not sex, significantly influenced GRIP1 expression. Indeed, GRIP1 expression was significantly higher in alpha-males (~22%)

compared to their subordinates, alpha-females were also found to have a relatively greater GRIP1 expression (~8%), though this was not a statistically significant difference.

The trafficking of AMPARs is highly regulated by protein-protein interactions, and plays a key role in synaptic plasticity, including long-term potentiation, which is characterized by increased synaptic strength. GRIP1 binds directly to GluA2 and GluA3 subunits, and work in cell culture has identified the role of GRIP1 in regulating the targeting of AMPARs to the synapse (Bissen et al., 2019; Chung et al., 2000; Tan et al., 2020). Previous work has found enhancement of synaptic, but not cellular, GRIP1 following chemically induced long-term potentiation, suggesting GRIP1 is recruited to synapses during LTP (Tan et al., 2020). In the same study, it was found that chemically induced LTP did not increase synaptic enrichment of AMPARs in GRIP1 knockout mice, suggesting GRIP1 is essential for AMPAR trafficking to the synapse during this form of plasticity (Tan et al., 2020).

Interestingly, Han et al., (2017) explored social behaviours of GRIP1/GRIP2 knockout male mice compared to wild type mice, as measured by a modified 3-chamber behavioural test. The researchers found the double knockout mice showed increased sociability and preference for social novelty compared to wild type mice (Han et al., 2017). Furthermore, the researchers assessed the amount of time mice spent interacting in pairs, and found that dyads of the double knockout mice spent significantly more time participating in non-aggressive behaviours compared to dyads of the wildtype mice (Han et al., 2017). Finally, the double knockout mice had significantly increased phosphorylation of the GluA2 Serine 880 residue, but not total GluA2 or PICK1, in the frontal cortex compared to wildtype mice. Phosphorylation of the

GluA2 Serine 880 residue by protein kinase C, reduces interactions between GluA2-GRIP1, but not GluA2-PICK1 (Chung et al., 2000; Terashima et al., 2004). Although the double knockout mice in the Han et al., (2017) study were found to have increased social behaviours, the lack of GRIP1 and the increase in phosphorylated Serine 880 suggests decreased synaptic expression of GluA2-containing AMPARs. When considering these findings in the context of our results, it is interesting that we observed dominant rats (both male and female) to exhibit greater total GluA2 and GRIP1 expression than their subordinate counterparts.

Interestingly, we found evidence for a small, but statistically significant, interaction effect of sex and social position in both PICK1 and stargazin expression. That is, the sex by position interaction for both PICK1 and stargazin was found to explain only ~1% of the total expression of these proteins. We hypothesized dominant animals would have decreased expression of PICK1, but increased expression of stargazin compared to their subordinates. With PICK1 we observed alpha-males to have greater expression than delta-males (~11%), however alpha- and delta-females had similar levels of expression. Regarding stargazin, alpha- and delta- males had somewhat similar levels of expression, while alpha-females had greater expression than their subordinates (~24%). As we observed a statistically significant interaction, it is difficult to interpret the relative contribution of sex and social position, our 2 factors, on the expression of these proteins.

As hypothesized, we found GRIP1 and stargazin expression to be increased in dominant animals as these proteins are involved in the trafficking, and stabilization of AMPAR receptors to the synapse. With regards to PICK1, we expected decreased levels in dominant

animals; however, we observed the opposite among male rats, and no difference in female rats. Taken together, our results suggest differences in the expression of proteins involved in AMPAR trafficking among dominant and subordinate animals, and the potential role of sex in mediating, at least some of, these differences.

5.4 Stress effects on social position and neural protein expression

The social environment has been identified as a stressor for group-living species, where both dominant and subordinate animals may experience stress, with the more stressed social position being a function of factors such as the species, hierarchy type, and dominance maintenance methods (Beery & Kaufer, 2015; Sapolsky, 2005). To assess the influence of sex and dominance rank on perceived stress levels, we measured basal corticosterone, given that CORT is the primary stress hormone in rodents, and has been commonly used to assess stress levels in laboratory rats. Corticosterone levels were approximately twice as high in female rats compared to male rats ($p < .05$), however, we did not find evidence that CORT levels significantly differed across social positions.

Regarding sex-specific differences in CORT between male and female rats, our results align with literature showing female rats have increased basal CORT levels compared to males (Griffin & Whitacre, 1991; J. Lu et al., 2015). Furthermore, the lack of differences observed in basal CORT levels between dominant and subordinate male laboratory rodents is largely consistent with previous work (Milewski et al., 2024; Varholick et al., 2019; Williamson, Lee, et al., 2019). Among male and female mice, fecal glucocorticoids were not significantly associated with dominance rank (determined by the Tube Test), however animals in hierarchies

with greater instability had increased levels of glucocorticoids compared to those in stable hierarchies (Varholick et al., 2019). Similarly, a recent preprint study by Milewiski et al. (2024) also found no differences in basal corticosterone levels (from trunk blood) among male mice, but did observe differences when examining hierarchy instability. Male mice were group-housed in sets of 4, allowed to form stable hierarchies, then underwent a social reorganization paradigm where mice were removed from their hierarchy and group-housed with unfamiliar animals of equivalent rank. Like our study, the authors found that an individual's social rank was not associated with basal plasma corticosterone levels. Interestingly, following social reorganization, mice that were initially in the alpha position experienced the greatest increase in plasma CORT (Milewski et al., 2024). These results suggest hierarchy instability is most stressful for dominant males, as they need to maintain their status.

Williamson and colleagues conducted two separate studies on male and female mice to determine factors associated with social position. Among group-housed, male mice no relationship between plasma CORT and social position was identified, however, alpha mice in hierarchies with high levels of despotism (greater power imbalance between highest and lowest ranked animals) exhibited slightly lower CORT levels (Williamson et al., 2017). In contrast, among female mice, subordinates were found to have greater plasma corticosterone levels compared to their more dominant counterparts (Williamson, Lee, et al., 2019). The differences in these findings suggest potential differences between male and female hierarchies and highlight the importance of studying female social dynamics. Notably, hierarchy instability is a known stressor for group-living species and hierarchy reorganization tends to increase stress

levels of dominant animals as they need to maintain their rank (Sapolsky, 2005). In our study, the rats were group-housed by sex for 2 weeks prior to undergoing behavioural testing, which likely provided a stable environment with few stressors. If we were to introduce factors contributing to an unstable environment (such as a novel conspecific), it is likely dominant male rats would experience increased CORT levels compared to their subordinates, at least until the hierarchy stabilized.

We did not find any of the neural proteins to be highly correlated with corticosterone levels. The lack of correlation was not surprising as we did not observe a significant difference in CORT levels across social position. The strongest relationships observed were among alpha-males (stargazin-CORT, r = -0.55), and delta-females (GRIP1-CORT, r = 0.58). Given that very few studies have explored AMPARs, their regulatory proteins, and stress in the context of social rank, making comparisons to the literature was difficult. When examining AMPAR phosphorylation in the context of dominance, male mice who underwent chronic restraint stress (and won fewer Tube Test matches), exhibited significantly decreased (~ less than 50%) total GluA2 expression, and decreased phosphorylation of Serine 818, and 831 on GluA1 (Park et al., 2018). Phosphorylation of these subunits was also found to be associated with winning points; that is, male mice who won more Tube Test matches had increased phosphorylation of these subunits, suggesting chronic stress caused social subordination, and AMPAR regulation differed between social ranks. Overall, the results of our study suggest the animals were not under sufficient stress to observe differences in CORT across social position, nor correlations among neural proteins.

5.5 Hierarchy linearity and neural protein expression

Finally, we examined how hierarchy linearity may influence neural protein expression as we were interested in whether differences between alpha and delta animals would be more apparent in hierarchies that were consistently linear. For our exploratory analysis, we only included male and female groups that remained linear throughout the duration of behavioural experiments, which provided us with a total of 4/10 male groups and 3/10 female groups. Among male rats, we did not observe a difference in expression of any of our proteins of interest. However, the practical significance, as measured by Cohen's d, was moderate-large for almost all of the proteins examined: GluA1 ($d = 0.61$), GluA2 ($d = 0.81$), GRIP1 ($d = 1.04$), and PICK1 ($d = 0.47$). In all cases, alpha-males had increased levels of the protein compared to subordinates. Among female animals, the alpha's were found to have significantly higher levels of stargazin expression compared to subordinates, and the effect size of the difference was considerable ($d = 2.02$). Although the comparison did not meet the threshold for statistical significance, the effect of social position on GluA2 expression among females was also very large ($d = 1.98$). Our results are consistent with the literature, in that male hierarchies tend to be more linear, despotic, and have greater power imbalances than female hierarchies (Williamson et al., 2016; Williamson, Lee, et al., 2019). Furthermore, observing large effect sizes in the absence of statistical significance suggests our sample size of stable groups was small, however, there appears to be a relationship between rank stability and expression of our proteins of interest, and the association may be more pronounced in male rats.

Chapter 6

Conclusions

6.1 Limitations

When interpreting the results of this study it is necessary to put our findings in the context of the study limitations. The main limitations that will be discussed are the lack of additional dominance tests to validate the Tube Test results, the way in which stress was assessed, and the use of whole tissue homogenates instead of synaptic tissue for our molecular analysis. The Tube Test is a reliable assay of social dominance where one animal has to "give way" to another, and has been used with both male and female rodents (Fan et al., 2019; Fulenwider et al., 2022). Ranks achieved from the Tube Test have been found to positively correlate with other dominance measures, such as the warm spot test and urine-marking assays (Šabanović et al., 2020; Wang et al., 2011). Additionally, this test is preferred over dominance assays that assess agonistic behaviours because it minimizes injury risk to the animals. However, animals undergoing the Tube Test are ranked based on pairwise interactions, while social hierarchies are formed under the broader social context of relationships between conspecifics. In other words, while dyadic assessments do provide information on individual-level interactions, they may not fully capture group-level dynamics (Strauss & Shizuka, 2022; Williamson et al., 2016). To address this concern, and increase our confidence that the dominance ranks from the Tube Test are valid, an additional dominance measure of resource competition among the group would be useful. The warm-spot test is a potential assay that

could be used, as dominance of cage-mates (not just dyads) could be assessed at the same time; however, this paradigm has not yet been fully characterized in female rats.

The second limitation that will be discussed is the use of plasma corticosterone to assess stress. Glucocorticoid levels, both cortisol and corticosterone, are known to fluctuate throughout the day with highest concentrations found in the morning (Greff et al., 2019; Windle et al., 1998). As such, collecting blood samples from rats essentially provides a snapshot of their levels of stress at the time of collection, but does not tell us about stress levels over a longer time scale. Of note, serum blood samples for all animals in our study were collected at the same time of day, therefore any fluctuations in CORT levels would be consistent across animals. As we did not find evidence that stress levels significantly differed between dominant and subordinate animals, our work suggests social position in this study was not a stressful experience for the animals.

Finally, the use of whole tissue homogenates from the mPFC limits our understanding of molecular differences across social position at the synapse. We found significant differences in GluA2, but not GluA1, subunit expression between dominant and subordinate animals; since these subunits are key players in synaptic plasticity, it would be interesting to explore their levels of synaptic expression. Furthermore, alpha males had increased GRIP1 and PICK1 expression compared to their subordinates, which was unexpected considering these proteins perform opposing roles in AMPAR trafficking. At the synapse, with increased AMPAR activity we would predict to see greater GRIP1 (and stargazin) expression compared to PICK1. Notably, we did see significant results in our analyses, suggesting whole tissue is sufficient to

explore AMPAR subunits and their associated auxiliary proteins in this context. Nevertheless, the use of synaptoneurosomes would provide further nuance about synaptic structure in these animals, and more clearly delineate molecular differences underlying male and female hierarchies.

6.2 Future directions and implications

To address the discussed limitations, future work should use an additional measure of social dominance, such as the warm-spot test, to validate dominance ranks from the Tube Test. Alternative methods to determine perceived stress could be done through the non-invasive assessment of corticosterone in fecal or fur samples. The measurement of fecal corticosterone metabolites would allow for the measurement of CORT levels at multiple time points throughout behavioural testing (Thanos et al., 2009). Additionally, fur corticosterone has been increasingly used as a marker for longer-term stress compared to serum CORT in rodents (Greff et al., 2019; Scorrano et al., 2015). The use of fur corticosterone would provide information on stress levels of the animals over a longer time scale, remove the potential confounding effect of diurnal CORT variation, and provide insight to potential stressors experienced during the shipping and husbandry process (which we attempted to account for through blocking). Furthermore, to understand molecular differences among dominant and subordinate animals at synaptic terminals, synaptic preparations (such as synaptoneurosomes) should be used.

Moreover, to understand the role of AMPAR trafficking, two additional molecular techniques should be used. First, the use of co-immunoprecipitation would identify direct

protein-protein interactions between AMPAR subunits and their associated proteins. AMPA receptors are heteromeric complexes surrounded by auxiliary proteins, fundamental to their regulation (Bessa-Neto & Choquet, 2023; Bissen et al., 2019). GRIP1 and PICK1 both bind the GluA2 subunit, and are involved in AMPAR insertion/stabilization, and removal, respectively. Stargazin binds to both GluA1 and GluA2, and is necessary for AMPAR stabilization at the postsynaptic density. The current study provides valuable insights to AMPAR subunit and auxiliary protein expression, however AMPA receptors do not exist in isolation at the synapse, so understanding the levels and types of protein-protein interactions in the context of dominance is crucial. The second technique that would expand upon the current work is the examination of phosphorylation sites on GluA1 and GluA2. Similar to Park et al. (2018), the Serine 818 and Serine 831 residues of GluA1 should be explored, as these were previously implicated in social dominance. Examination of these sites would contribute to the literature by providing data on basal levels of phosphorylation as opposed to the stress-induced changes observed by Park et al. (2018). Since phosphorylation of the Serine 880 site on GluA2 is a key regulator of how the subunit interacts with GRIP1 and PICK1, examining this residue would also provide additional important information about AMPAR trafficking.

The final recommendation for future studies is to examine expression of GluA1, GluA2, GRIP1, PICK1, and stargazin among all hierarchy members. To further our understanding of social interactions within a hierarchy, future work should include not only the highest and lowest ranked animals, but the middle ones as well. As this was an exploratory study, we chose to explore neural protein differences among the most dominant (alpha) and

the least dominant (delta) animals, because if there were to be differences in neural protein expression across social rank, we expected that they would be most obvious between alpha and delta animals. Our study provides evidence to suggest there are differences in neural protein expression among alpha and delta animals, some of which differ by sex, however the interactions and behaviours of these animals occur within the broader context of their social environment, so examination of neural protein expression among middle ranked animals will provide information on the nuances of dominance rank.

Our results provide evidence that social position significantly influences GluA2 and GRIP1 expression in the medial prefrontal cortex of male and female rats. Furthermore, expression of PICK1 and stargazin are modulated through a sex by position interaction. In addition, we did not find evidence that stress levels differed between the highest and lowest ranked animals. Differences in AMPAR subunit and auxiliary protein expression among dominant and subordinate animals is noteworthy due to the known role of AMPAR dysregulation in various brain disorders. As the main mediators of fast, excitatory transmission, the role of AMPA receptor function in neurodevelopmental and neurodegenerative disorders, such as autism spectrum disorder and Alzheimer's disease, is of great interest. Social dominance hierarchies are ubiquitous among group-living species and the present study adds to the literature on male-male and female-female dynamics in rats, and provides the first report on whether the expression of AMPAR subunits and their key regulatory proteins are changed through social position.

Tables and Figures

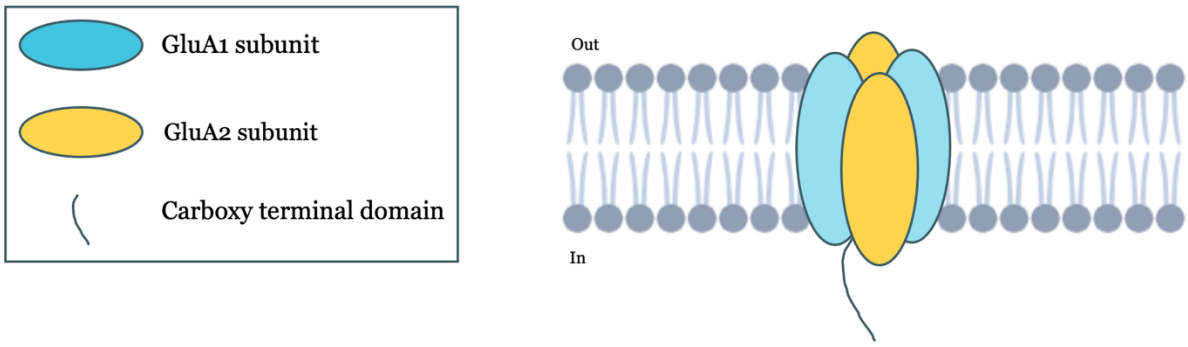


Figure 1. AMPA receptor embedded in the post-synaptic membrane.

The AMPA receptor is a tetrameric complex comprised of a set of dimers. The majority of AMPARs contain either GluA1 or GluA2. The current figure shows one representative carboxy terminal domain (CTD), however each AMPA subunit has a CTD region.

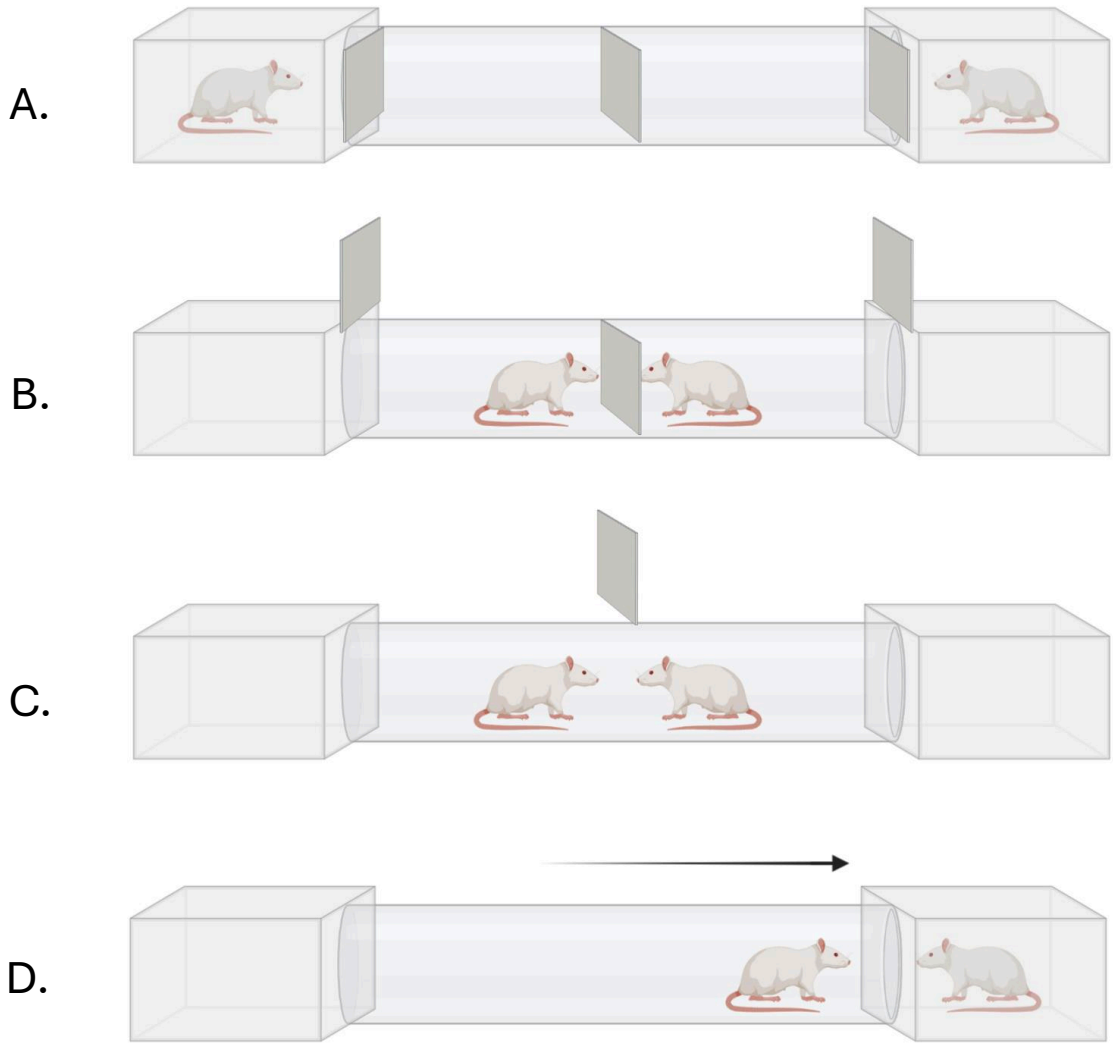


Figure 2. Tube Test schematic.

A) The rats began in the holding cages with all three doors closed. B) The doors separating the holding cages from the tube were removed, allowing the animals to move to the middle of the tube. C) Once the animals reached the middle of the tube, the middle door was removed, and the trial began. D) The animal that pushed the other back into its holding cage was designated as the winner of the trial. Created with BioRender.com.

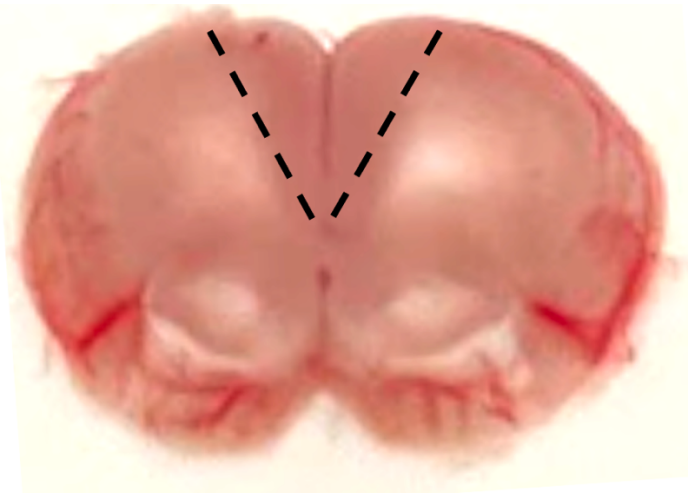


Figure 3. Coronal slice of a typical rat brain at the level used for the dissection (rostral view).

The area inside the dashed lines indicates where the medial prefrontal cortex was dissected.

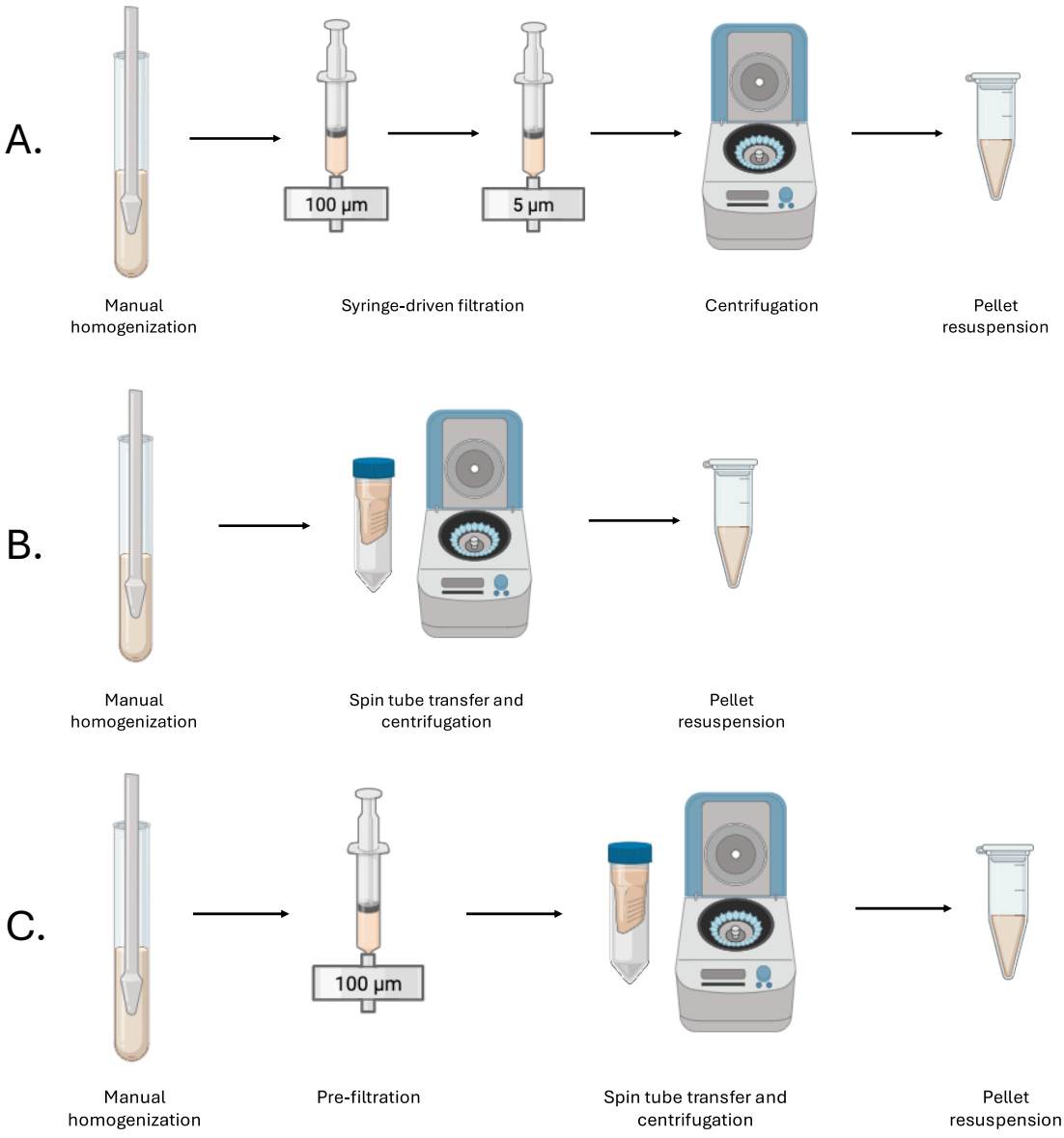


Figure 4. Synaptoneurosome protocols.

A) 2-step syringe-driven method. B) Centrifuge-driven spin tube method. C) Centrifuge-driven spin tube method with pre-filtration. Created with BioRender.com.

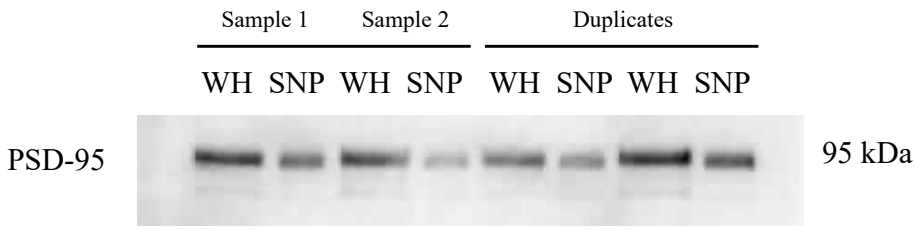


Figure 5. Characterization of SNPs using 0.5 mL spin tubes.

Medial PFC tissue was used to determine the effectiveness of the spin tube method to prepare synaptoneurosomes using 0.5 mL spin tubes. The tissue was homogenized then split into two 0.5 mL spin tubes and samples were spun at 15,000 x g for 5 mins at 4°C, then combined and resuspended. The blot shows PSD-95 (95 kDa) expression in WH and SNP. Relative expression of the SNP bands is less than the WH indicating lack of synaptic enrichment. PFC, prefrontal cortex; SNP, synaptoneurosome preparation; WH, whole homogenate

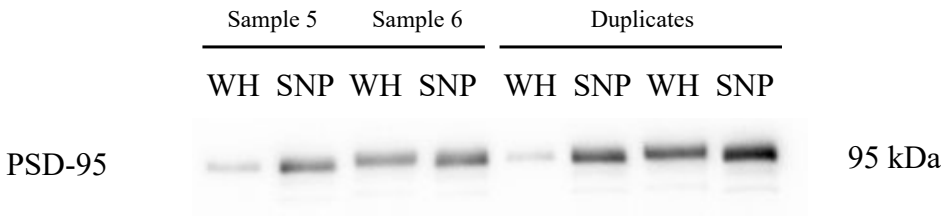


Figure 6. Characterisation of SNPs using a 2 mL spin tube with, or without filtration.

Medial PFC tissue was used to determine the effectiveness of the spin tube method to prepare synaptoneurosomes using 2 mL spin tubes. Samples were spun at 3,200 x g for 15 mins at room temperature. Sample 5 was filtered prior to placement in the spin tube (see Figure 4C) and Sample 6 was not pre-filtered. The blot shows PSD-95 (95 kDa) expression in WH and SNP from both samples. Relative expression of PSD-95 in the SNPs is greater than the WH indicating synaptic enrichment was achieved with both methods, however, enrichment was qualitatively greater when pre-filtration was used. PFC, prefrontal cortex; SNP, synaptoneurosome preparation; WH, whole homogenate

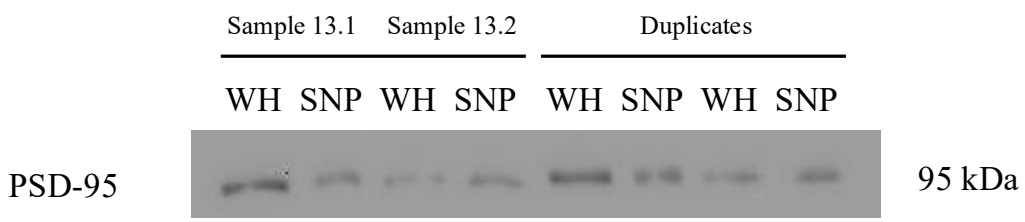


Figure 7. Characterisation of SNPs using a 2 mL spin tube with pre-filtration.

Medial PFC and septal hippocampal tissue were used to determine the effectiveness of the spin tube method to prepare synaptoneurosomes using 2 mL spin tubes. Samples were spun at 3,200 x g for 15 mins at room temperature. Sample 13.1 is the mPFC and Sample 13.2 is the septal hippocampus from the same animal. The blot shows PSD-95 (95 kDa) expression in both WH and SNP. Relative expression of the SNP bands of Sample 13.1 less than the WH indicating synaptic enrichment was not achieved. PFC, prefrontal cortex; SNP, synaptoneurosome preparation; WH, whole homogenate

Sample ID	Region	Spin Tube(s)	Pre-Filtration	Spin Speed (x g)	Spin Time (min)	Spin Temp. (°C)	Enrichment
1	mPFC	Two 0.5 ml tubes	No	15,000	5	4	-
2	mPFC	Two 0.5 ml tubes	No	15,000	5	4	-
3	mPFC	0.5 ml	No	15,000	5	4	-
4	mPFC	Two 0.5 ml tubes	No	15,000	5	4	-
5	mPFC	2 ml	Yes	3,200	15	20	+++
6	mPFC	2 ml	No	3,200	15	20	++
7	mPFC	2 ml	Yes	3,500	15	4	-
8	mPFC	2 ml	Yes	3,500	15	4	+
9	mPFC	2 ml	No	3,500	15	4	-
10	mPFC	2 ml	No	3,500 & 1000*	20+5	4	-
11	mPFC	2 ml	No	3,500 & 1000*	25	20	-
12.1	Septal left	2 ml	Yes	3,200	15	4	+++
12.2	Septal right	2 ml	Yes	3,200	15	20	++
13.1	mPFC	2 ml	Yes	3,200	15	20	-
13.2	Septal left	2 ml	Yes	3,200	15	20	+++
14.1	mPFC	2 ml	Yes	3,200	15	20	+
14.2	Septal left	2 ml	Yes	3,200	15	20	-
15.1	mPFC	2 ml	Yes	3,200	15	20	+
15.2	Septal left	2 ml	Yes	3,200	15	20	+

Table 1. Summary of SNP characterisation results

When characterizing the SNP protocol, variables including tissue type, use of spin tubes, pre-filtration, and centrifuge conditions were altered. (-) indicates no enrichment, and "plus signs" indicate low ("+", 1.1-1.3x), moderate ("++", 1.4-1.9x), and high ("+++", >2x) levels of PSD-95 enrichment. *Samples were spun sequentially at 3,500 x g and then 1,000 x g.

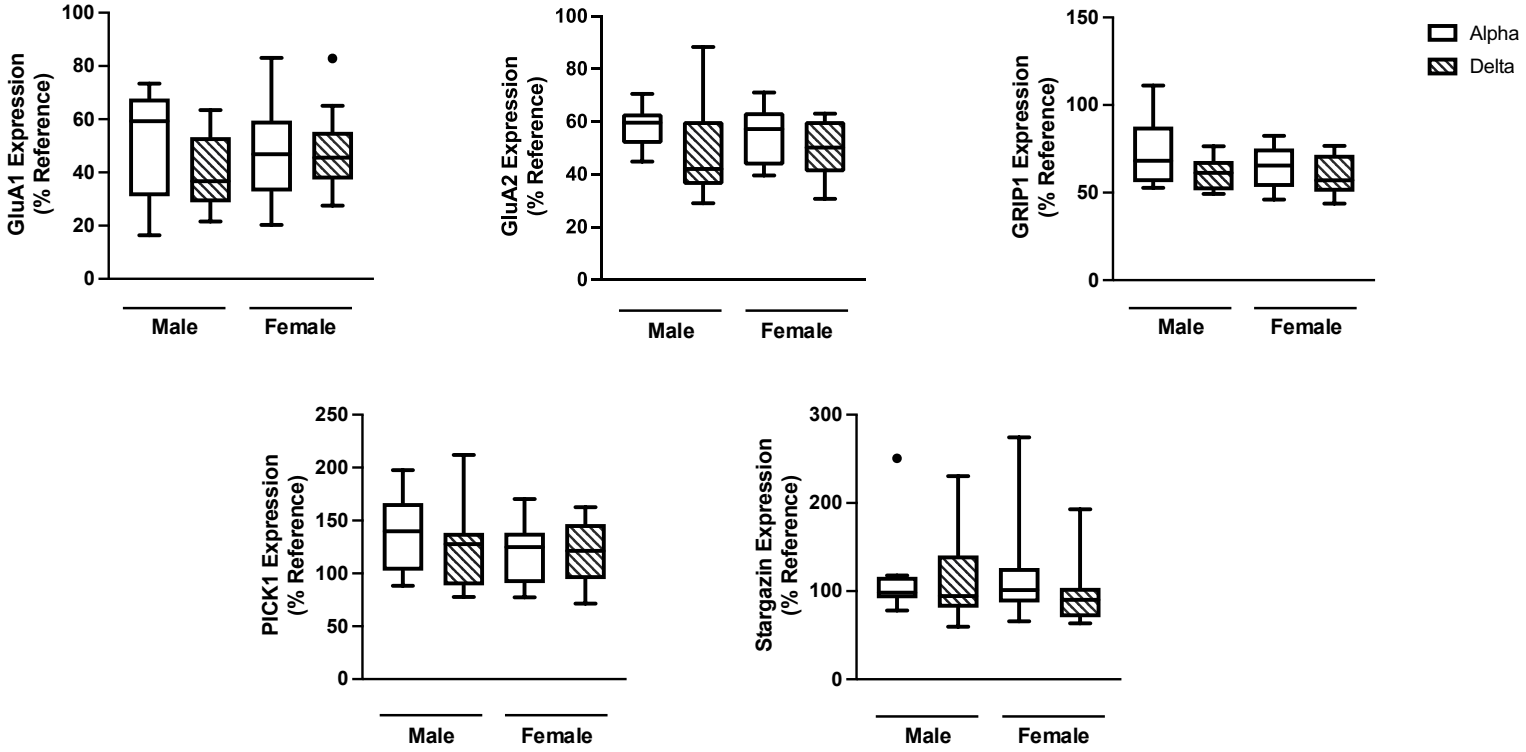


Figure 8. Box and whisker plots using Tukey's method to identify outliers within neural protein data.

Two outliers were identified, one in the female GluA1 group, and one among the male stargazin group. The horizontal line in each box reflects the median value.

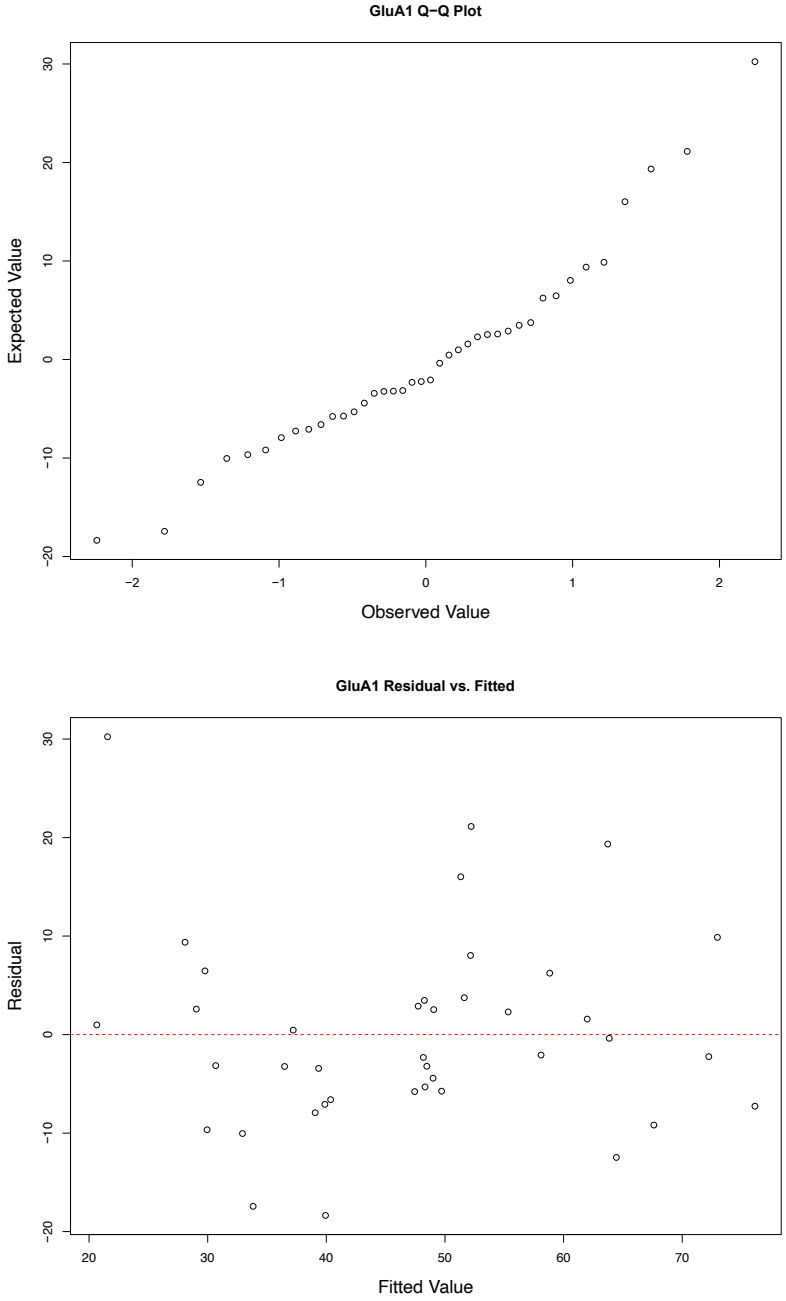


Figure 9. Diagnostic plots for GluA1.

Upper figure is a Q-Q plot of the residuals for GluA1. Lower figure is the Residual versus Fitted plot for GluA1.

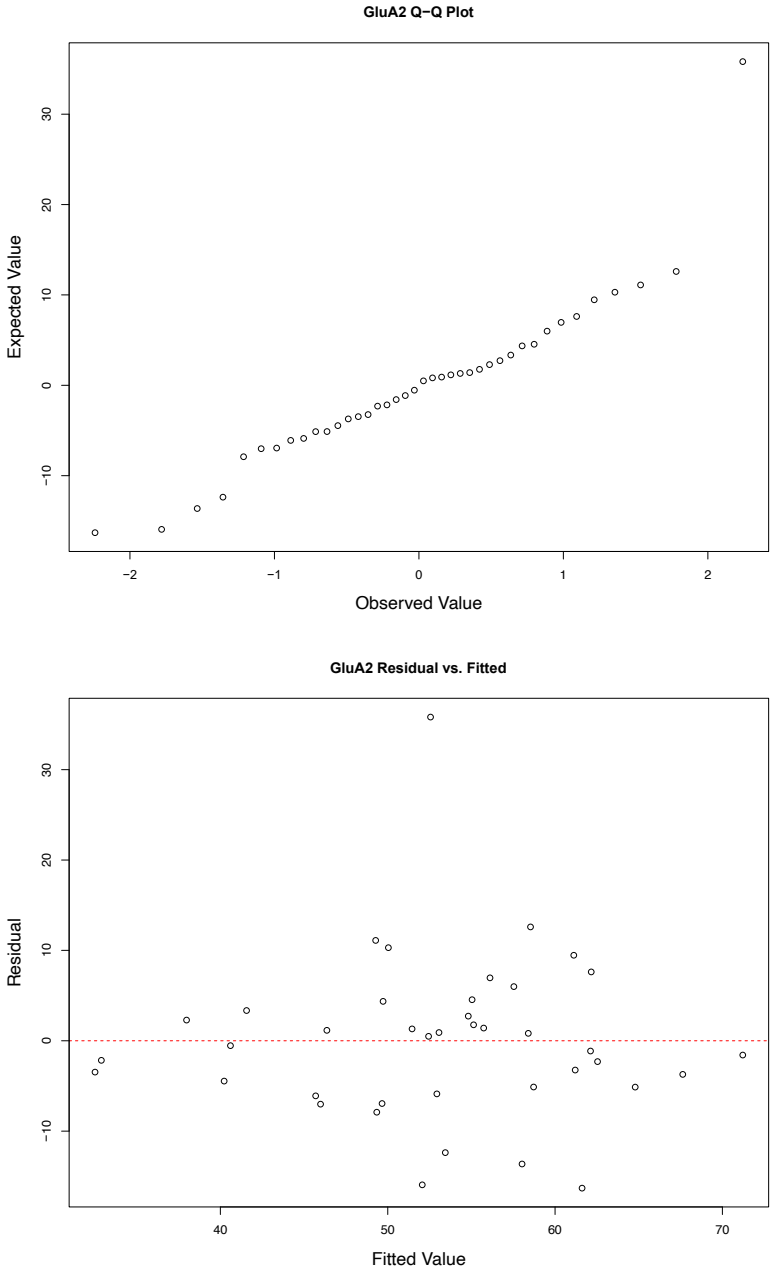


Figure 10. Diagnostic plots for GluA2.

Upper figure is a Q-Q plot of the residuals for GluA2. Lower figure is the Residual versus Fitted plot for GluA2.

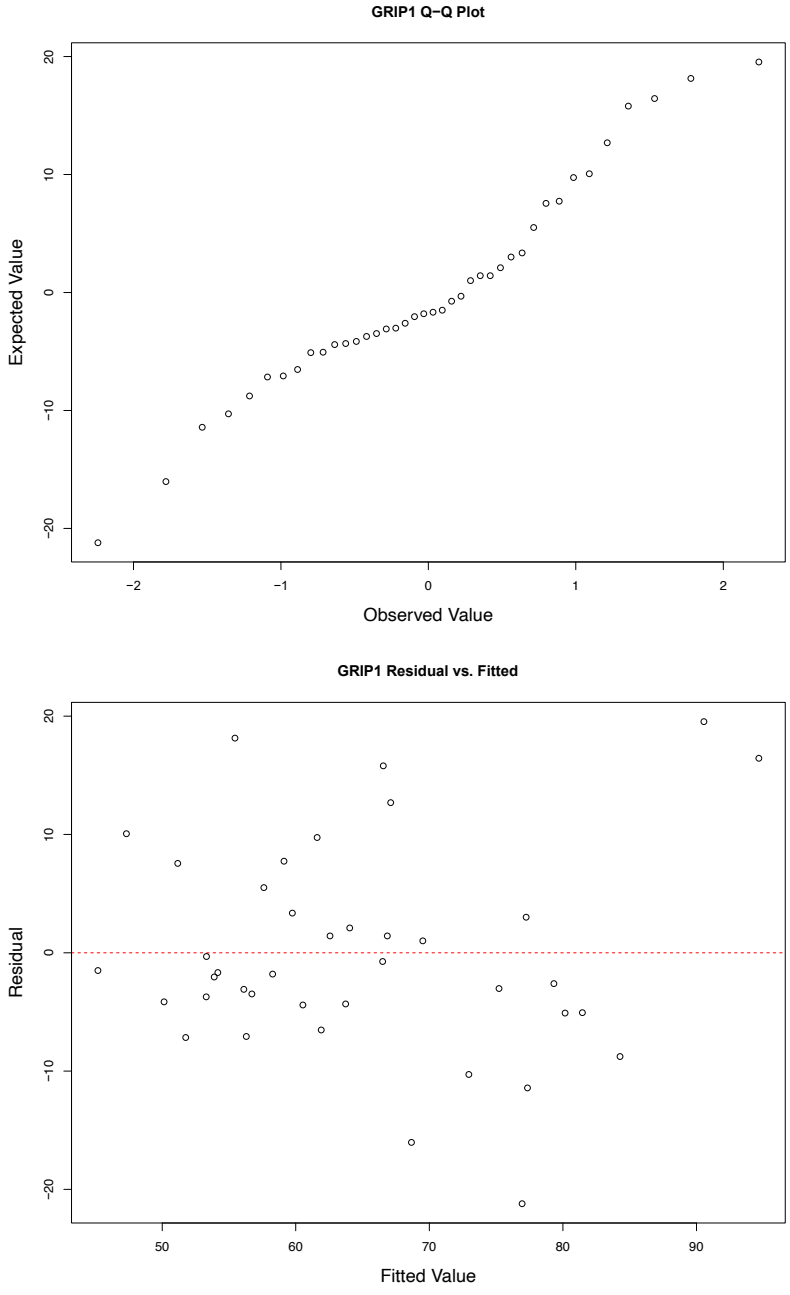


Figure 11. Diagnostic plots for GRIP1.

Upper figure is a Q-Q plot of the residuals for GRIP1. Lower figure is the Residual versus Fitted plot for GRIP1.

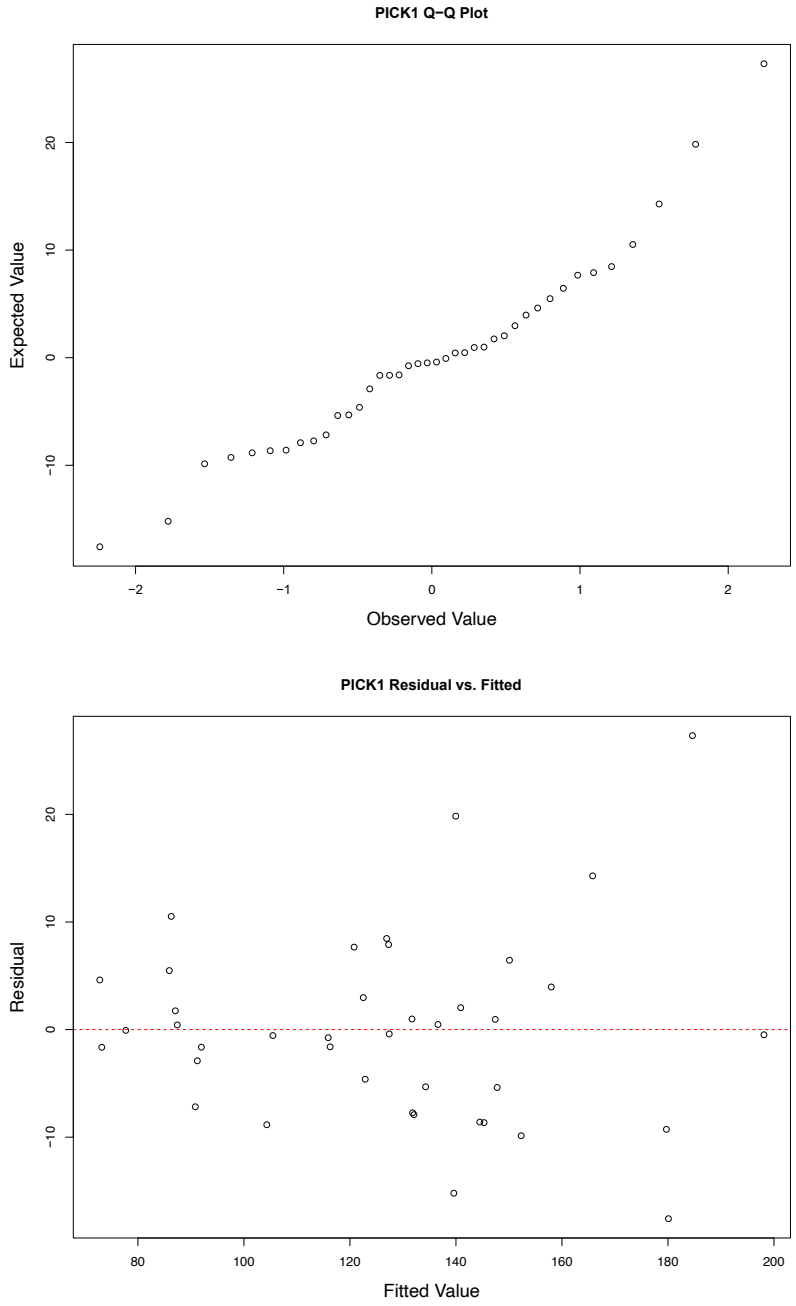


Figure 12. Diagnostic plots for PICK1.

Upper figure is a Q-Q plot of the residuals for PICK1. Lower figure is the Residual versus Fitted plot for PICK1.

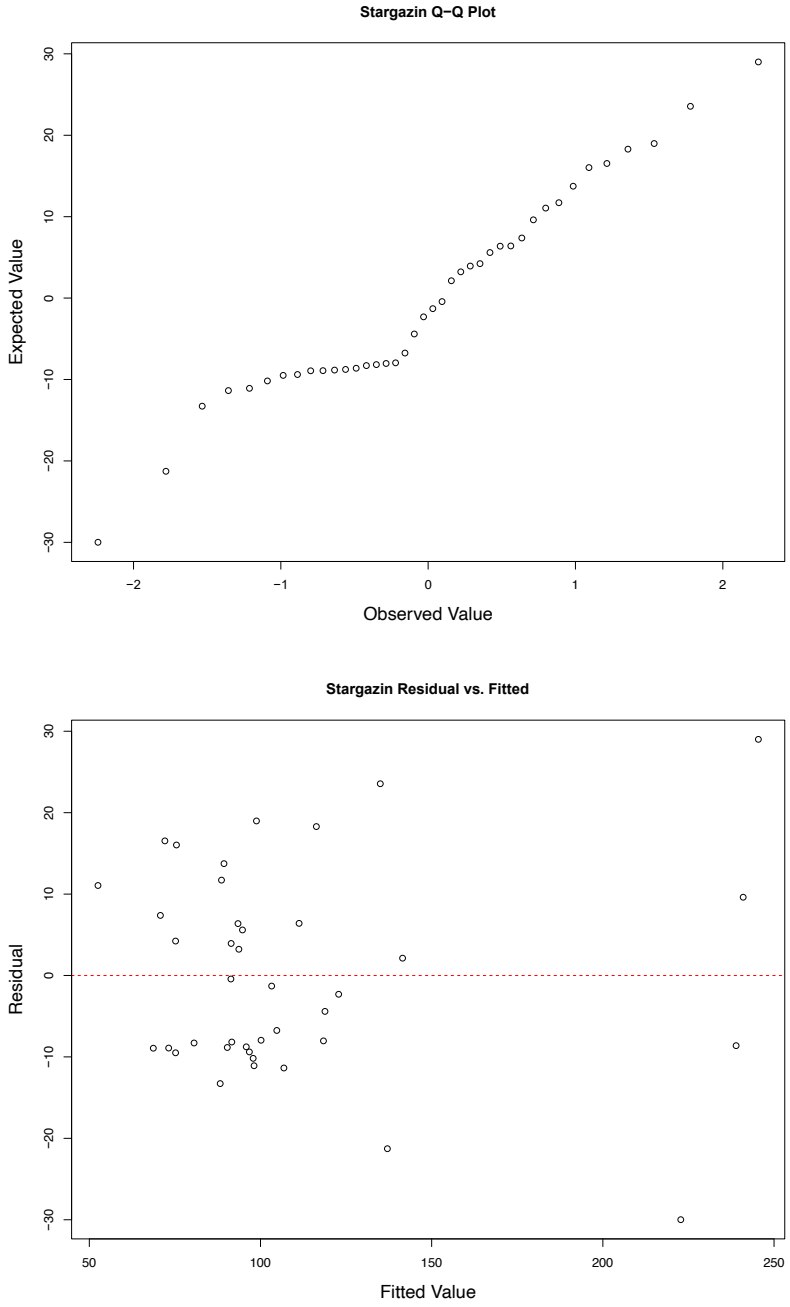


Figure 13. Diagnostic plots for Stargazin.

Upper figure is a Q-Q plot of the residuals for stargazin. Lower figure is the Residual versus Fitted plot for stargazin.

	Df	Sum Sq	Mean Sq	F value	p-value	Eta-squared
Sex	1	68.4	68.41	0.48	.494	.006
Position	1	333.3	333.28	2.35	.137	.029
Sex*Position	1	422.8	422.81	1.98	.096	.036
Residuals	27	3834.5	142.02			

Table 2. Summary of two-factor ANOVA test for GluA1.

The effects of sex, position, and their interaction on GluA1 expression in the medial prefrontal cortex was examined. Df, degrees of freedom; Sq, square



Figure 14. GluA1 expression in the medial prefrontal cortex of dominant and subordinate male and female rats.

A) The summary plot presents the expression of GluA1 in the medial prefrontal cortex of dominant (alpha) and subordinate (delta) rats, stratified by sex, N = 10 groups. The values for each sample were normalized to the reference value (whole prefrontal cortex) on their respective blots. The data are expressed as mean ± SEM. B) Representative immunoblot image of GluA1 expression (~100 kDa) in the medial PFC. α, alpha; δ, delta; Ref, reference sample

	Df	Sum Sq	Mean Sq	F value	p-value	Eta-squared
Sex	1	25.7	25.73	0.22	.644	.004
Position	1	500.3	500.32	4.23	.049	.081
Sex*Position	1	39.3	39.26	0.33	.569	.006
Residuals	27	3190.1	118.15			

Table 3. Summary of two-factor ANOVA test for GluA2

The effects of sex, position, and their interaction on GluA2 expression in the medial prefrontal cortex was examined. Df, degrees of freedom; Sq, square

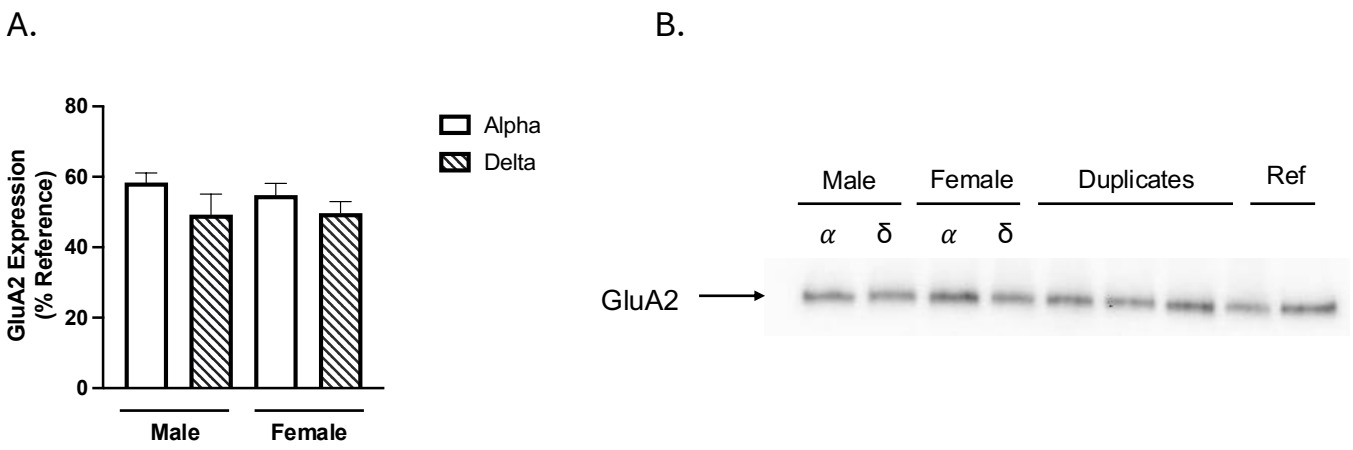


Figure 15. GluA2 expression in the medial prefrontal cortex of dominant and subordinate male and female rats.

A) The summary plot presents the expression of GluA2 in the medial prefrontal cortex of dominant (alpha) and subordinate (delta) rats, stratified by sex, N = 10 groups. The values for each sample were normalized to the reference value (whole prefrontal cortex) on their respective blots. The data are expressed as mean ± SEM. B) Representative immunoblot image of GluA2 expression (~100 kDa) in the medial PFC. α, alpha; δ, delta; Ref, reference sample

	Df	Sum Sq	Mean Sq	F value	p-value	Eta-squared
Sex	1	392.3	392.29	3.42	.076	.045
Position	1	824.7	824.68	7.18	.012	.095
Sex*Position	1	170.6	170.58	1.49	.233	.020
Residuals	27	3100.9	114.85			

Table 4. Summary of two-factor ANOVA test for GRIP1.

The effects of sex, position, and their interaction on GRIP1 expression in the medial prefrontal cortex was examined. Df, degrees of freedom; Sq, square

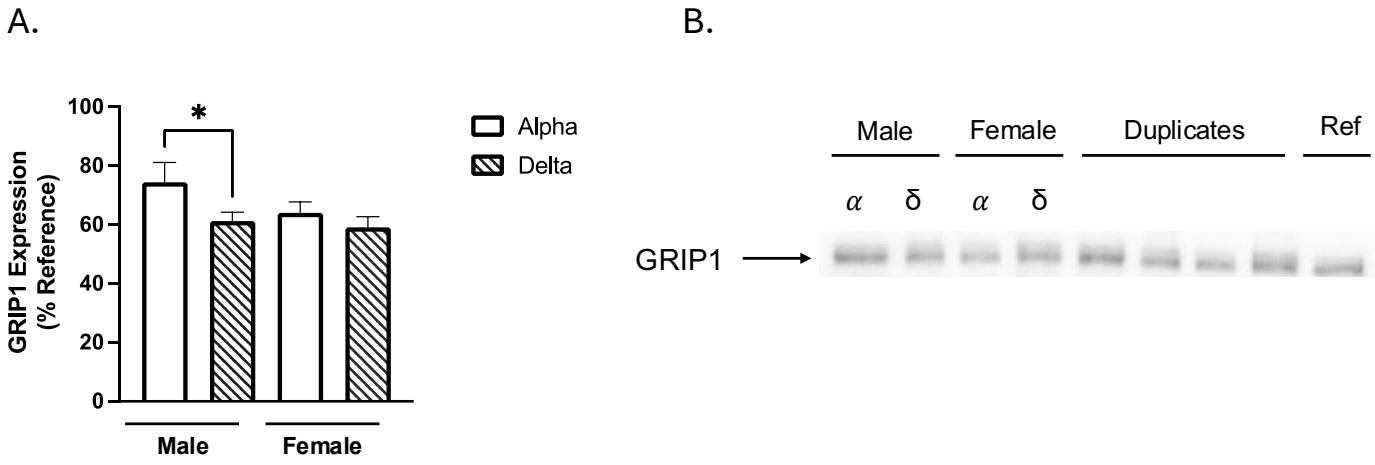


Figure 16. GRIP1 expression in the medial prefrontal cortex of dominant and subordinate male and female rats.

A) The summary plot presents the expression of GRIP1 in the medial prefrontal cortex of dominant (alpha) and subordinate (delta) rats, stratified by sex, N = 10 groups. The values for each sample were normalized to the reference value (whole prefrontal cortex) on their respective blots. The data are expressed as mean ± SEM. B) Representative immunoblot image of GRIP1 expression (~130 kDa) in the medial PFC. α, alpha; δ, delta; Ref, reference sample

* Indicates a significant pair-wise comparison using Tukey's HSD ($p < .05$).

Sex	Position	Mean GluA2 Expression (%Reference)	Standard deviation	p-value	Cohen's d
Males	Alpha	58.39	8.60	.267	0.634
	Delta	49.33	18.29		
Females	Alpha	54.80	10.55	.723	0.486
	Delta	49.71	10.39		

Table 5. Summary of Tukey's HSD comparing between group differences in GluA2 expression among male and female animals.

Rats were stratified by sex, then compared for significant differences in GluA2 levels between alphas and deltas.

Sex	Position	Mean GRIP1 Expression (%Reference)	Standard deviation	p-value	Cohen's d
Males	Alpha	74.47	21.26	.048	0.802
	Delta	61.26	9.54		
Females	Alpha	64.08	11.72	.731	0.427
	Delta	59.12	11.50		

Table 6. Summary of Tukey's HSD comparing between group differences in GRIP1 expression among male and female animals.

Rats were stratified by sex, then compared for significant differences in GRIP1 levels between alphas and deltas.

	Df	Sum Sq	Mean Sq	F value	p-value	Eta-squared
Sex	1	1313	1313.4	11.85	.002	.031
Position	1	430	430.3	3.88	.059	.010
Sex*Position	1	480	479.9	4.33	.047	.011
Residuals	27	2994	110.9			

Table 7. Summary of two-factor ANOVA test for PICK1.

The effects of sex, position, and their interaction on PICK1 expression in the medial prefrontal cortex was examined. Df, degrees of freedom; Sq, square

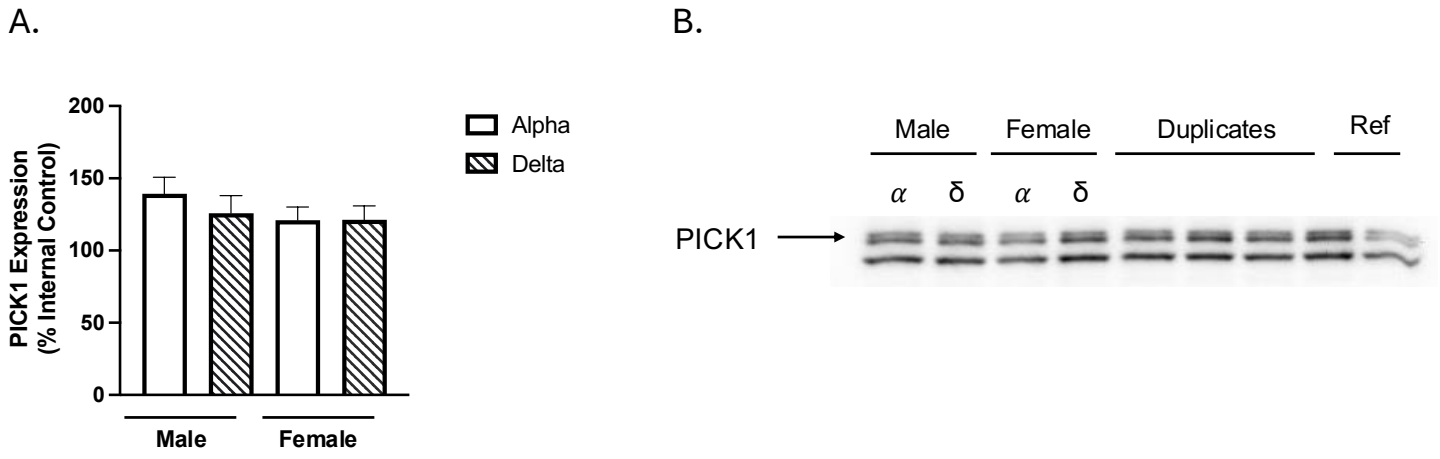


Figure 17. PICK1 expression in the medial prefrontal cortex of dominant and subordinate male and female rats.

A) The summary plot presents the expression of PICK1 in the medial prefrontal cortex of dominant (alpha) and subordinate (delta) rats, stratified by sex, N = 10 groups. The values for each sample were normalized to the reference value (whole prefrontal cortex) on their respective blots. The data are expressed as mean ± SEM. A significant sex by position interaction was observed from the two-way ANOVA analysis. B) Representative immunoblot image of PICK1 expression (~52 kDa) in the medial PFC. α, alpha; δ, delta; Ref, reference sample

	Df	Sum Sq	Mean Sq	F value	p-value	Eta-squared
Sex	1	343	343.5	1.50	.231	.004
Position	1	1530	1529.8	6.70	.015	.017
Sex*Position	1	1060	1060.0	4.64	.040	.012
Residuals	27	6163	228.3			

Table 8. Summary of two-factor ANOVA test for Stargazin.

The effects of sex, position, and their interaction on stargazin expression in the medial prefrontal cortex was examined. Df, degrees of freedom; Sq, square

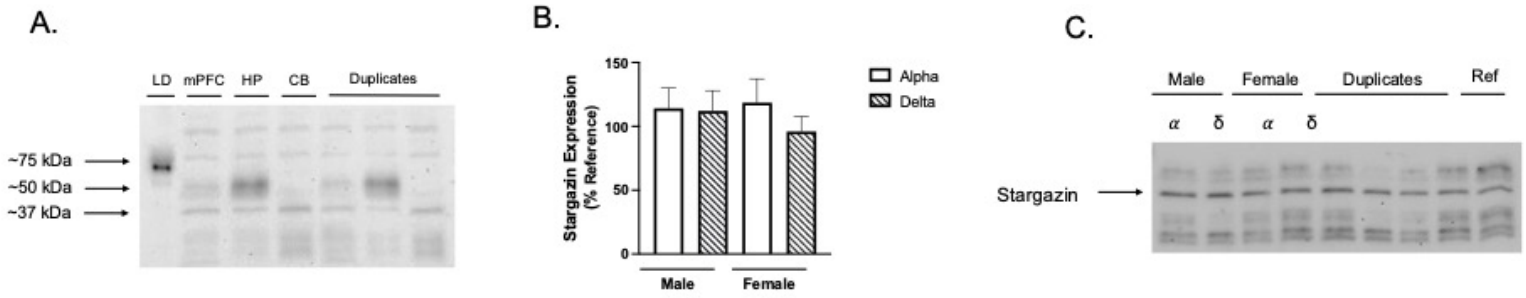


Figure 18. Stargazin expression in the medial prefrontal cortex of dominant and subordinate male and female rats.

A) Results from a positive control test that examined the expression of stargazin in the medial prefrontal cortex, hippocampus, and cerebellum. The primary TARP found in the CB is stargazin (TARP γ-2), found at ~37 kDa, whereas the primary TARP in the HP, TARP γ-8, is found at ~50 kDa and absent in the CB. The blot confirms the presence of stargazin within the mPFC at ~37 kDa, which was the band used for analysis. B) The summary plot presents the expression of Stargazin in the medial prefrontal cortex of dominant (alpha) and subordinate (delta) rats, stratified by sex, N = 10 groups. The values for each sample were normalized to the reference value (whole prefrontal cortex) on their respective blots. The data are expressed as mean $\pm$ SEM. A significant sex by position interaction was observed from the two-way ANOVA analysis. C) Representative immunoblot image of Stargazin expression in the medial PFC. α, alpha; δ, delta; CB, cerebellum; HP, hippocampus; LD, ladder; mPFC, medial prefrontal cortex; Ref, reference sample

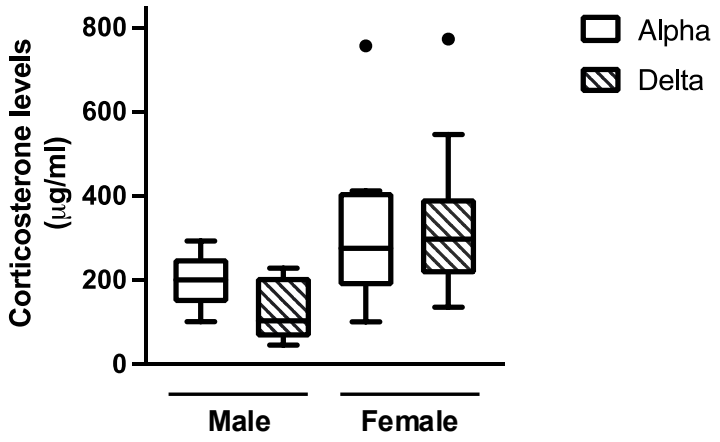


Figure 19. Box and whisker plot using Tukey's method to identify outliers in corticosterone data.

Two outliers were identified, one in the alpha-female, and one in the delta-female group. The horizontal line in each box reflects the median value.

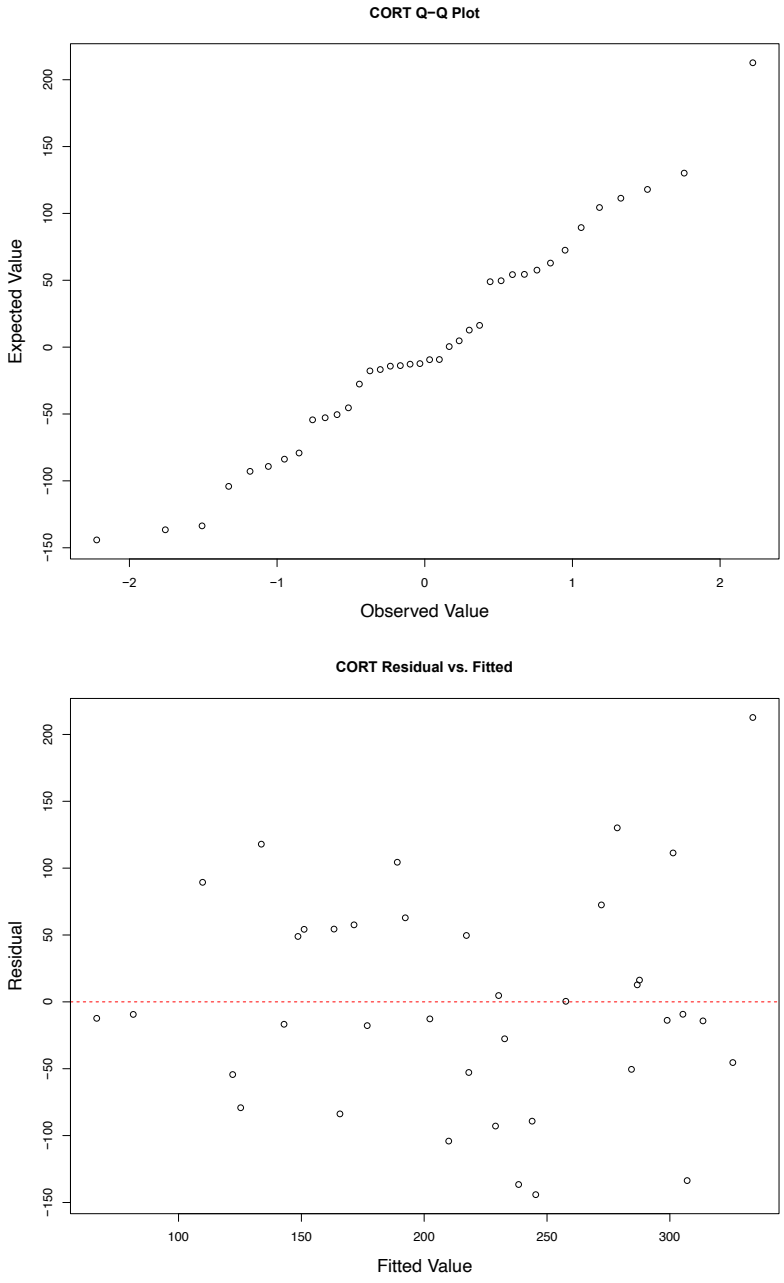


Figure 20. Diagnostic plots for corticosterone levels.

Upper figure is a Q-Q plot of the residuals for corticosterone. Lower figure is the Residual versus Fitted plot for corticosterone. Data presented is without two outliers.

	Df	Sum Sq	Mean Sq	F value	p-value	Eta-squared
Sex	1	122557	122557	12.68	.002	.287
Position	1	5813	5813	0.60	.445	.012
Sex*Position	1	20405	20405	2.11	.159	.047
Residuals	25	241693	9668			

Table 9. Summary of two-factor ANOVA test of corticosterone levels.

Rats were compared for significant differences in corticosterone levels by examining the effects of sex, position, and their interaction.

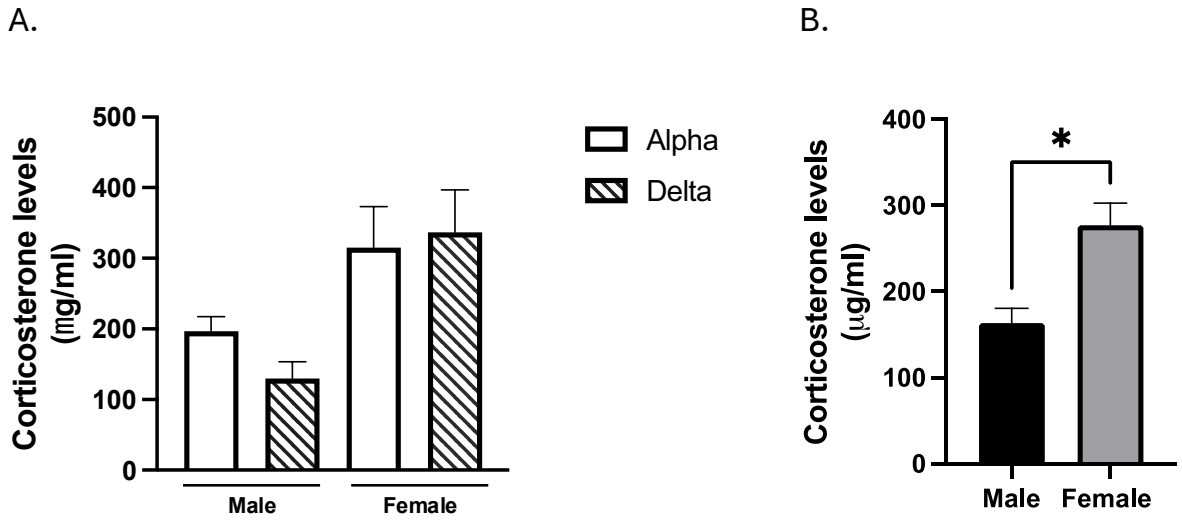


Figure 21. Differences in corticosterone levels between male and female rats.

A) The summary plot presents corticosterone levels of the animals measured from trunk blood, N = 10 groups (removed 2 outliers). B) Female rats were found to have corticosterone levels approximately twice the amount observed in males.

* Indicates a significant effect of sex from two-factor ANOVA ($p < .05$)

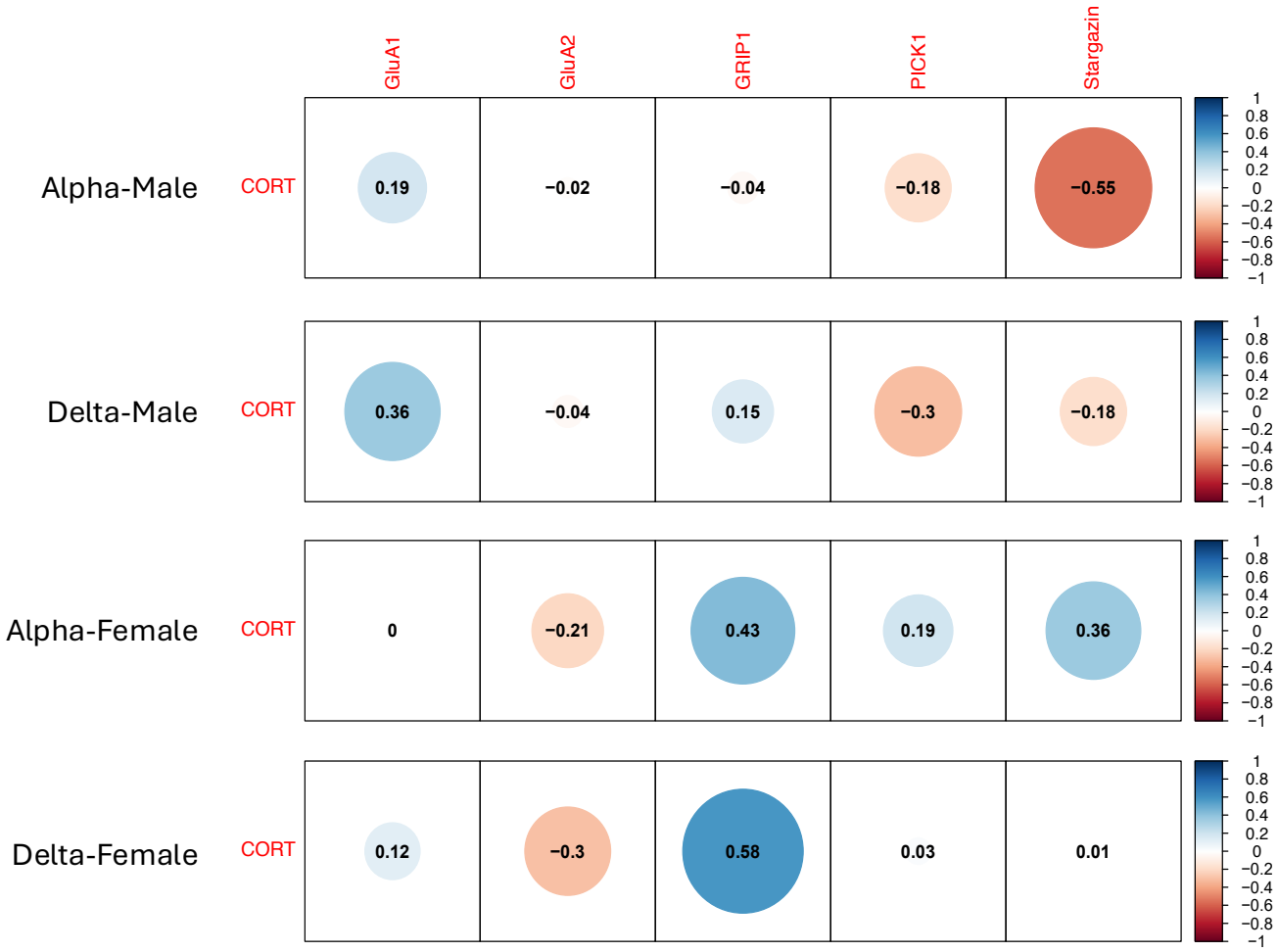


Figure 22. Correlation matrix of the relationship between corticosterone levels and neural protein expression among subgroup of interest.

A correlation matrix depicting the correlation between corticosterone levels and neural protein expression among alpha-males, delta-males, alpha-females, and delta-females. Blue dots indicate a positive relationship, red dots indicate a negative relationship with darker dots representing a higher level of correlation. The Pearson correlation coefficient (r) is presented in black in the center of each box.

		Df	Sum Sq	Mean Sq	F value	p-value	Cohen's d
Males	**Position**	1	187.17	187.17	1.14	.363	0.609
	Residuals	3	490.66	163.55			
Females	**Position**	1	54.49	54.49	0.23	.679	0.309
	Residuals	2	475.07	237.54			

Table 10. Summary of one-way ANOVA test of only linear, male and female groups for GluA1.

Male and female rats were separately compared for significant differences in GluA1 expression in the medial prefrontal cortex by examining the effect of position. N of males = 4 groups, N of females = 3 groups.

		Df	Sum Sq	Mean Sq	F value	p-value	Cohen's d
Males	**Position**	1	144.53	144.53	2.33	.225	0.813
	Residuals	3	186.44	62.148			
Females	**Position**	1	327.67	327.67	3.50	.203	1.976
	Residuals	2	187.25	93.62			

Table 11. Summary of one-way ANOVA test of only linear, male and female groups for GluA2.

Male and female rats were separately compared for significant differences in GluA2 expression in the medial prefrontal cortex by examining the effect of position. N of males = 4 groups, N of females = 3 groups.

		Df	Sum Sq	Mean Sq	F value	p-value	Cohen's d
Males	**Position**	1	203.74	203.74	2.13	.241	1.038
	Residuals	3	287.55	95.85			
Females	**Position**	1	54.45	54.45	3.07	.222	0.407
	Residuals	2	35.51	17.76			

Table 12. Summary of one-way ANOVA test of only linear, male and female groups for GRIP1.

Male and female rats were separately compared for significant differences in GRIP1 expression in the medial prefrontal cortex by examining the effect of position. N of males = 4 groups, N of females = 3 groups.

		Df	Sum Sq	Mean Sq	F value	p-value	Cohen's d
Males	**Position**	1	229.14	229.14	9.33	.055	0.470
	Residuals	3	73.70	24.57			
Females	**Position**	1	2.16	2.16	0.09	.794	0.068
	Residuals	2	48.82	24.41			

Table 13. Summary of one-way ANOVA test of only linear, male and female groups for PICK1.

Male and female rats were separately compared for significant differences in PICK1 expression in the medial prefrontal cortex by examining the effect of position. N of males = 4 groups, N of females = 3 groups.

		Df	Sum Sq	Mean Sq	F value	p-value	Cohen's d
Males	**Position**	1	2.46	2.46	0.02	.904	0.072
	Residuals	3	424.97	141.66			
Females	**Position**	1	945.57	945.57	41.46	.023	2.024
	Residuals	2	45.61	22.80			

Table 14. Summary of one-way ANOVA test of only linear, male and female groups for Stargazin.

Male and female rats were separately compared for significant differences in Stargazin expression in the medial prefrontal cortex by examining the effect of position. N of males = 4 groups, N of females = 3 groups.

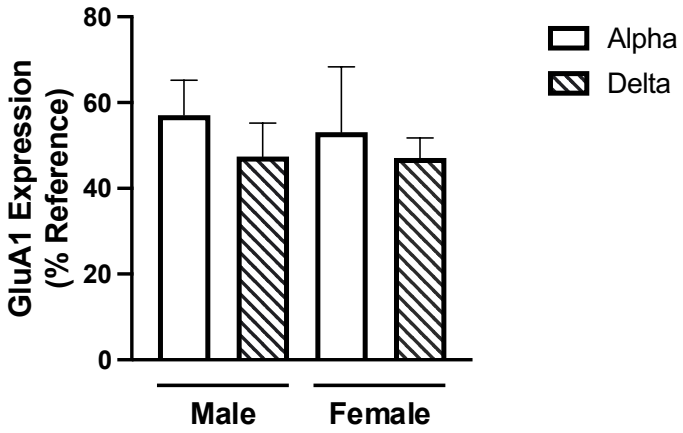


Figure 23. GluA1 expression in the medial prefrontal cortex of dominant and subordinate male and female rats from stable, linear hierarchies.

The summary plot presents the expression of GluA1 in the medial prefrontal cortex of dominant (alpha) and subordinate (delta) rats, stratified by sex from only linear hierarchies. Four male groups and three female groups are presented. The values for each sample were normalized to the reference value (whole prefrontal cortex) on their respective blots. The data are expressed as mean $\pm$ SEM.

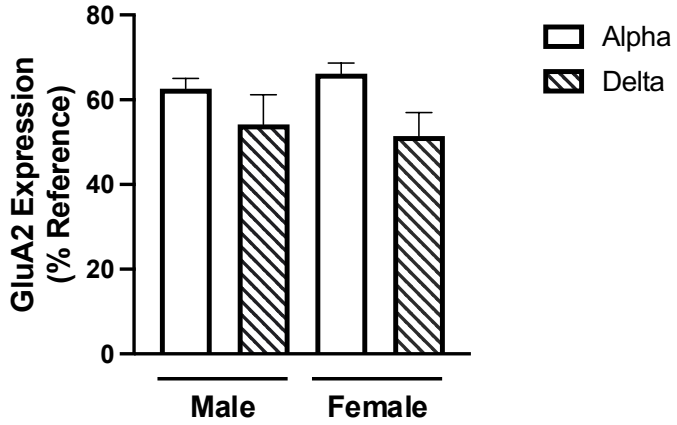


Figure 24. GluA2 expression in the medial prefrontal cortex of dominant and subordinate male and female rats from stable, linear hierarchies.

The summary plot presents the expression of GluA2 in the medial prefrontal cortex of dominant (alpha) and subordinate (delta) rats, stratified by sex from only linear hierarchies. Four male groups and three female groups are presented. The values for each sample were normalized to the reference value (whole prefrontal cortex) on their respective blots. The data are expressed as mean $\pm$ SEM.

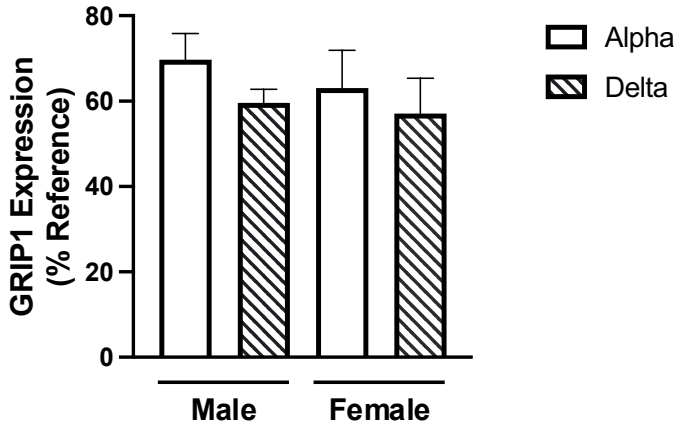


Figure 25. GRIP1 expression in the medial prefrontal cortex of dominant and subordinate male and female rats from stable, linear hierarchies.

The summary plot presents the expression of GRIP1 in the medial prefrontal cortex of dominant (alpha) and subordinate (delta) rats, stratified by sex from only linear hierarchies. Four male groups and three female groups are presented. The values for each sample were normalized to the reference value (whole prefrontal cortex) on their respective blots. The data are expressed as mean $\pm$ SEM.

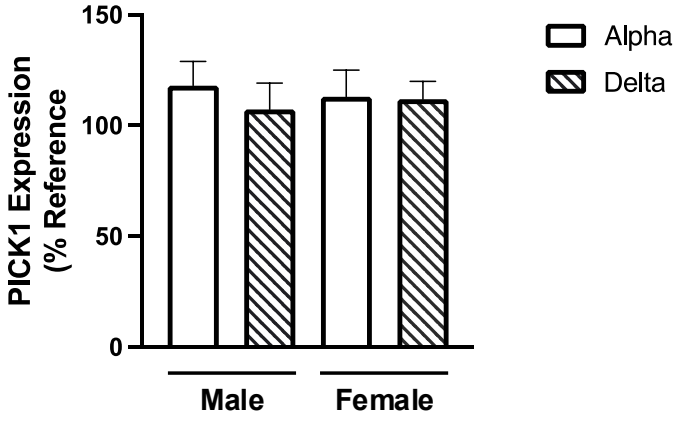


Figure 26. PICK1 expression in the medial prefrontal cortex of dominant and subordinate male and female rats from stable, linear hierarchies.

The summary plot presents the expression of PICK1 in the medial prefrontal cortex of dominant (alpha) and subordinate (delta) rats, stratified by sex from only linear hierarchies. Four male groups and three female groups are presented. The values for each sample were normalized to the reference value (whole prefrontal cortex) on their respective blots. The data are expressed as mean $\pm$ SEM.

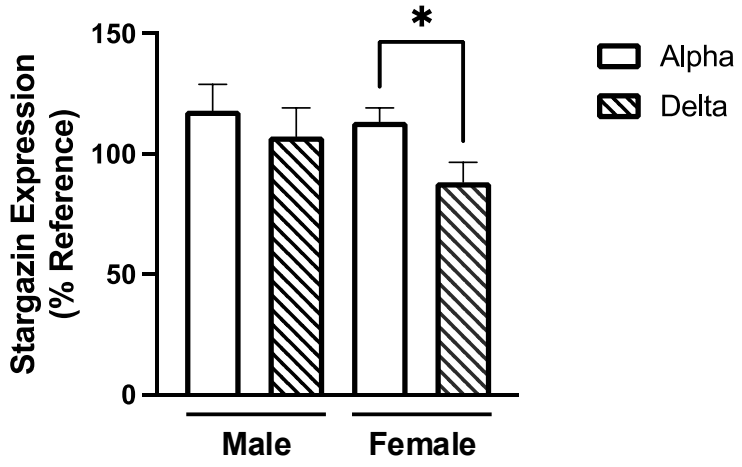


Figure 27. Stargazin expression in the medial prefrontal cortex of dominant and subordinate male and female rats from stable, linear hierarchies.

The summary plot presents the expression of stargazin in the medial prefrontal cortex of dominant (alpha) and subordinate (delta) rats, stratified by sex from only linear hierarchies. Four male groups and three female groups are presented. The values for each sample were normalized to the reference value (whole prefrontal cortex) on their respective blots. The data are expressed as mean $\pm$ SEM.

* Indicates a significant effect of sex from one-factor ANOVA ($p < .05$)

References

Anacker, A., & Beery, A. (2013). Life in groups: The roles of oxytocin in mammalian sociality. *Frontiers in Behavioral Neuroscience*, *7*. https://www.frontiersin.org/articles/10.3389/fnbeh.2013.00185

Beery, A. K., & Kaufer, D. (2015). Stress, social behavior, and resilience: Insights from rodents. *Neurobiology of Stress*, *1*, 116–127. https://doi.org/10.1016/j.ynstr.2014.10.004

Belle, S. V., Estrada, A., Ziegler, T. E., & Strier, K. B. (2009). Social and hormonal mechanisms underlying male reproductive strategies in black howler monkeys (Alouatta pigra). *Hormones and Behavior*, *56*(4), 355–363. https://doi.org/10.1016/j.yhbeh.2009.08.006

Bercovitch, F. B., & Clarke, A. S. (1995). Dominance rank, cortisol concentrations, and reproductive maturation in male rhesus macaques. *Physiology & Behavior*, *58*(2), 215–221. https://doi.org/10.1016/0031-9384(95)00055-n

Bessa-Neto, D., & Choquet, D. (2023). Molecular mechanisms of AMPAR reversible stabilization at synapses. *Molecular and Cellular Neuroscience*, *125*, 103856. https://doi.org/10.1016/j.mcn.2023.103856

Bissen, D., Foss, F., & Acker-Palmer, A. (2019). AMPA receptors and their minions: Auxiliary proteins in AMPA receptor trafficking. *Cellular and Molecular Life Sciences*, *76*(11), 2133–2169. Scopus. https://doi.org/10.1007/s00018-019-03068-7

Blanchard, D. C., Cholvanich, P., Blanchard, R. J., Clow, D. W., Hammer, R. P., Rowlett, J. K., & Bardo, M. T. (1991). Serotonin, but not dopamine, metabolites are increased in selected brain regions of subordinate male rats in a colony environment. *Brain Research*, *568*(1–2), 61–66. https://doi.org/10.1016/0006-8993(91)91379-F

Bredt, D. S., & Nicoll, R. A. (2003). AMPA receptor trafficking at excitatory synapses. *Neuron*, *40*(2), 361–379. Scopus. https://doi.org/10.1016/S0896-6273(03)00640-8

Bushnik, T., Tjepkema, M., & Martel, L. (2020). Socioeconomic disparities in life and health expectancy among the household population in Canada. *Health Reports*, *31*(1), 3–14. https://doi.org/10.25318/82-003-x202000100001-eng

Chase, I. D., Tovey, C., Spangler-Martin, D., & Manfredonia, M. (2002). Individual differences versus social dynamics in the formation of animal dominance hierarchies. *Proceedings of the National Academy of Sciences*, *99*(8), 5744–5749. https://doi.org/10.1073/pnas.082104199

Chelini, M. O. M., Palme, R., & Otta, E. (2011). Social stress and reproductive success in the female Syrian hamster: Endocrine and behavioral correlates. *Physiology & Behavior*, *104*(5), 948–954. https://doi.org/10.1016/j.physbeh.2011.06.006

Chen, E., & Miller, G. E. (2013). Socioeconomic Status and Health: Mediating and Moderating Factors. *Annual Review of Clinical Psychology*, *9*(1), 723–749. https://doi.org/10.1146/annurev-clinpsy-050212-185634

Chung, H. J., Xia, J., Scannevin, R. H., Zhang, X., & Huganir, R. L. (2000). Phosphorylation of the AMPA Receptor Subunit GluR2 Differentially Regulates Its Interaction with

PDZ Domain-Containing Proteins. *The Journal of Neuroscience*, *20*(19), 7258–7267. https://doi.org/10.1523/JNEUROSCI.20-19-07258.2000

Cooper, M. A., Seddighi, S., Barnes, A. K., Grizzell, J. A., Dulka, B. N., & Clinard, C. T. (2017). Dominance status alters restraint-induced neural activity in brain regions controlling stress vulnerability. *Physiology & Behavior*, *179*, 153–161. https://doi.org/10.1016/j.physbeh.2017.06.003

Creel, S. (2001). Social dominance and stress hormones. *Trends in Ecology & Evolution*, *16*(9), 491–497. https://doi.org/10.1016/S0169-5347(01)02227-3

Davari, S., D'Costa, N., Ramezan, R., & Mielke, J. G. (2023). Chronic early-life social isolation enhances spatial memory in male and female rats. *Behavioural Brain Research*, *447*, 114433. https://doi.org/10.1016/j.bbr.2023.114433

de Vries, H., Stevens, J. M. G., & Vervaecke, H. (2006). Measuring and testing the steepness of dominance hierarchies. *Animal Behaviour*, *71*(3), 585–592. https://doi.org/10.1016/j.anbehav.2005.05.015

Díaz-Alonso, J., & Nicoll, R. A. (2021). AMPA receptor trafficking and LTP: Carboxy-termini, amino-termini and TARPs. *Neuropharmacology*, *197*. Scopus. https://doi.org/10.1016/j.neuropharm.2021.108710

Drews, C. (1993). The Concept and Definition of Dominance in Animal Behaviour. *Behaviour*, *125*(3/4), 283–313.

Dulka, B. N., Bress, K. S., Grizzell, J. A., & Cooper, M. A. (2018). Social Dominance Modulates Stress-induced Neural Activity in Medial Prefrontal Cortex Projections to

the Basolateral Amygdala. *Neuroscience*, *388*, 274–283. https://doi.org/10.1016/j.neuroscience.2018.07.042

Fan, Z., Zhu, H., Zhou, T., Wang, S., Wu, Y., & Hu, H. (2019). Using the tube test to measure social hierarchy in mice. *Nature Protocols*, *14*(3), Article 3. https://doi.org/10.1038/s41596-018-0116-4

Franklin, T. B., Silva, B. A., Perova, Z., Marrone, L., Masferrer, M. E., Zhan, Y., Kaplan, A., Greetham, L., Verrechia, V., Halman, A., Pagella, S., Vyssotski, A. L., Illarionova, A., Grinevich, V., Branco, T., & Gross, C. T. (2017). Prefrontal cortical control of a brainstem social behavior circuit. *Nature Neuroscience*, *20*(2), Article 2. https://doi.org/10.1038/nn.4470

Fulenwider, H. D., Caruso, M. A., & Ryabinin, A. E. (2022). Manifestations of domination: Assessments of social dominance in rodents. *Genes, Brain and Behavior*, *21*(3). Scopus. https://doi.org/10.1111/gbb.12731

Fuster, J. (2015). *The Prefrontal Cortex*. Academic Press.

Gangopadhyay, P., Chawla, M., Monte, O. D., & Chang, S. W. C. (2021). Prefrontal-Amygdala Circuits in Social Decision-Making. *Nature Neuroscience*, *24*(1), 5–18. https://doi.org/10.1038/s41593-020-00738-9

Garcia-Font, N., Mitchell-Heggs, R., Saxena, K., Gabbert, C., Taylor, G., Mastroberardino, G., Spooner, P. A., Gobbo, F., Dabrowska, J. K., Chattarji, S., Kind, P. C., Schultz, S. R., & Morris, R. G. M. (2022). Ca2+ imaging of self and other in medial prefrontal cortex during social dominance interactions in a tube test. *Proceedings of the National*

Academy of Sciences, *119*(31), e2107942119. https://doi.org/10.1073/pnas.2107942119

Gaskill, B. N., & Garner, J. P. (2020). Power to the People: Power, Negative Results and Sample Size. *Journal of the American Association for Laboratory Animal Science : JAALAS*, *59*(1), 9–16. https://doi.org/10.30802/AALAS-JAALAS-19-000042

Gow, R., Koren, G., Rieder, M., & Van Uum, S. (2011). Hair cortisol content in patients with adrenal insufficiency on hydrocortisone replacement therapy. *Clinical Endocrinology*, *74*(6), 687–693. https://doi.org/10.1111/j.1365-2265.2011.04001.x

Greenberg, G. D., Howerton, C. L., & Trainor, B. C. (2014). Fighting in the home cage: Agonistic encounters and effects on neurobiological markers within the social decision-making network of house mice (Mus musculus). *Neuroscience Letters*, *566*, 151–155. Scopus. https://doi.org/10.1016/j.neulet.2014.02.051

Greff, M. J. E., Levine, J. M., Abuzgaia, A. M., Elzagallaai, A. A., Rieder, M. J., & van Uum, S. H. M. (2019). Hair cortisol analysis: An update on methodological considerations and clinical applications. *Clinical Biochemistry*, *63*, 1–9. https://doi.org/10.1016/j.clinbiochem.2018.09.010

Griffin, A. C., & Whitacre, C. C. (1991). Sex and strain differences in the circadian rhythm fluctuation of endocrine and immune function in the rat: Implications for rodent models of autoimmune disease. *Journal of Neuroimmunology*, *35*(1–3), 53–64. https://doi.org/10.1016/0165-5728(91)90161-Y

Hajizadeh, M., Mitnitski, A., & Rockwood, K. (2016). Socioeconomic gradient in health in Canada: Is the gap widening or narrowing? *Health Policy*, *120*(9), 1040–1050. https://doi.org/10.1016/j.healthpol.2016.07.019

Han, M., Mejias, R., Chiu, S.-L., Rose, R., Adamczyk, A., Huganir, R., & Wang, T. (2017). Mice lacking GRIP1/2 show increased social interactions and enhanced phosphorylation at GluA2-S880. *Behavioural Brain Research*, *321*, 176–184. Scopus. https://doi.org/10.1016/j.bbr.2016.12.042

Hanley, J. G. (2008). PICK1: A multi-talented modulator of AMPA receptor trafficking. *Pharmacology and Therapeutics*, *118*(1), 152–160. Scopus. https://doi.org/10.1016/j.pharmthera.2008.02.002

Hansen, K. B., Wollmuth, L. P., Bowie, D., Furukawa, H., Menniti, F. S., Sobolevsky, A. I., Swanson, G. T., Swanger, S. A., Greger, I. H., Nakagawa, T., McBain, C. J., Jayaraman, V., Low, C.-M., Dell'Acqua, M. L., Diamond, J. S., Camp, C. R., Perszyk, R. E., Yuan, H., & Traynelis, S. F. (2021). Structure, Function, and Pharmacology of Glutamate Receptor Ion Channels. *Pharmacological Reviews*, *73*(4), 1469–1658. https://doi.org/10.1124/pharmrev.120.000131

Henley, J. M., & Wilkinson, K. A. (2016). Synaptic AMPA receptor composition in development, plasticity and disease. *Nature Reviews Neuroscience*, *17*(6), 337–350. Scopus. https://doi.org/10.1038/nrn.2016.37

Hertzman, C. (2012). Putting the concept of biological embedding in historical perspective. *Proceedings of the National Academy of Sciences*, *109*(supplement_2), 17160–17167. https://doi.org/10.1073/pnas.1202203109

Hollingsworth, E., McNeal, E., Burton, J., Williams, R., Daly, J., & Creveling, C. (1985). Biochemical characterization of a filtered synaptoneurosome preparation from guinea pig cerebral cortex: Cyclic adenosine 3':5'-monophosphate- generating systems, receptors, and enzymes. *The Journal of Neuroscience*, *5*(8), 2240–2253. https://doi.org/10.1523/JNEUROSCI.05-08-02240.1985

Isaac, J. T. R., Ashby, M. C., & McBain, C. J. (2007). The role of the GluR2 subunit in AMPA receptor function and synaptic plasticity. *Neuron*, *54*(6), 859–871. https://doi.org/10.1016/j.neuron.2007.06.001

Janet, R., Ligneul, R., Losecaat-Vermeer, A. B., Philippe, R., Bellucci, G., Derrington, E., Park, S. Q., & Dreher, J.-C. (2022). Regulation of social hierarchy learning by serotonin transporter availability. *Neuropsychopharmacology*, *47*(13), Article 13. https://doi.org/10.1038/s41386-022-01378-2

Joëls, M., Karst, H., & Sarabdjitsingh, R. A. (2018). The stressed brain of humans and rodents. *Acta Physiologica*, *223*(2), e13066. https://doi.org/10.1111/apha.13066

Kaplan, J. R., Manuck, S. B., Fontenot, M. B., & Mann, J. J. (2002). Central nervous system monoamine correlates of social dominance in cynomolgus monkeys (Macaca fascicularis). *Neuropsychopharmacology*, *26*(4), 431–443. Scopus. https://doi.org/10.1016/S0893-133X(01)00344-X

Karamihalev, S., Brivio, E., Flachskamm, C., Stoffel, R., Schmidt, M. V., & Chen, A. (2020). Social dominance mediates behavioral adaptation to chronic stress in a sex-specific manner. *eLife*, *9*, e58723. https://doi.org/10.7554/eLife.58723

Kesner, R. P., & Churchwell, J. C. (2011). An analysis of rat prefrontal cortex in mediating executive function. *Neurobiology of Learning and Memory*, *96*(3), 417–431. https://doi.org/10.1016/j.nlm.2011.07.002

Kim, E. J., Pellman, B., & Kim, J. J. (2015). Stress effects on the hippocampus: A critical review. *Learning & Memory*, *22*(9), 411–416. https://doi.org/10.1101/lm.037291.114

Kim, H.-Y. (2015). Statistical notes for clinical researchers: Post-hoc multiple comparisons. *Restorative Dentistry & Endodontics*, *40*(2), 172–176. https://doi.org/10.5395/rde.2015.40.2.172

Kiser, D., SteemerS, B., Branchi, I., & Homberg, J. R. (2012). The reciprocal interaction between serotonin and social behaviour. *Neuroscience & Biobehavioral Reviews*, *36*(2), 786–798. https://doi.org/10.1016/j.neubiorev.2011.12.009

Knight, E. L., & Mehta, P. H. (2017). Hierarchy stability moderates the effect of status on stress and performance in humans. *Proceedings of the National Academy of Sciences*, *114*(1), 78–83. https://doi.org/10.1073/pnas.1609811114

Knouse, M. C., McGrath, A. G., Deutschmann, A. U., Rich, M. T., Zallar, L. J., Rajadhyaksha, A. M., & Briand, L. A. (2022). Sex differences in the medial prefrontal cortical glutamate system. *Biology of Sex Differences*, *13*, 66. https://doi.org/10.1186/s13293-022-00468-6

Koert, A., Ploeger, A., Bockting, C. L. H., Schmidt, M. V., Lucassen, P. J., Schrantee, A., & Mul, J. D. (2021). The social instability stress paradigm in rat and mouse: A systematic review of protocols, limitations, and recommendations. *Neurobiology of Stress*, *15*, 100410. https://doi.org/10.1016/j.ynstr.2021.100410

Kolk, S. M., & Rakic, P. (2022). Development of prefrontal cortex. *Neuropsychopharmacology*, *47*(1), Article 1. https://doi.org/10.1038/s41386-021-01137-9

Koski, J., Xie, H., & Olson, I. R. (2015). Understanding Social Hierarchies: The Neural and Psychological Foundations of Status Perception. *Social Neuroscience*, *10*(5), 527–550. https://doi.org/10.1080/17470919.2015.1013223

Lakens, D. (2013). Calculating and reporting effect sizes to facilitate cumulative science: A practical primer for t-tests and ANOVAs. *Frontiers in Psychology*, *4*, 863. https://doi.org/10.3389/fpsyg.2013.00863

Lee, E., Rhim, I., Lee, J. W., Ghim, J.-W., Lee, S., Kim, E., & Jung, M. W. (2016). Enhanced Neuronal Activity in the Medial Prefrontal Cortex during Social Approach Behavior. *Journal of Neuroscience*, *36*(26), 6926–6936. https://doi.org/10.1523/JNEUROSCI.0307-16.2016

Lee, W., Dowd, H. N., Nikain, C., Dwortz, M. F., Yang, E. D., & Curley, J. P. (2021). Effect of relative social rank within a social hierarchy on neural activation in response to familiar or unfamiliar social signals. *Scientific Reports*, *11*(1), Article 1. https://doi.org/10.1038/s41598-021-82255-8

Lee, W., Hiura, L. C., Yang, E., Broekman, K. A., Ophir, A. G., & Curley, J. P. (2019). Social status in mouse social hierarchies is associated with variation in oxytocin and vasopressin 1a receptor densities. *Hormones and Behavior*, *114*, 104551. https://doi.org/10.1016/j.yhbeh.2019.06.015

Lu, J., Wu, X.-Y., Zhu, Q.-B., Li, J., Shi, L.-G., Wu, J.-L., Zhang, Q.-J., Huang, M.-L., & Bao, A.-M. (2015). Sex differences in the stress response in SD rats. *Behavioural Brain Research*, *284*, 231–237. https://doi.org/10.1016/j.bbr.2015.02.009

Lu, W., Shi, Y., Jackson, A. C., Bjorgan, K., During, M. J., Sprengel, R., Seeburg, P. H., & Nicoll, R. A. (2009). Subunit composition of synaptic AMPA receptors revealed by a single-cell genetic approach. *Neuron*, *62*(2), 254–268. https://doi.org/10.1016/j.neuron.2009.02.027

Malinow, R., & Malenka, R. C. (2002). AMPA receptor trafficking and synaptic plasticity. *Annual Review of Neuroscience*, *25*, 103–126. Scopus. https://doi.org/10.1146/annurev.neuro.25.112701.142758

Marcondes, L. A., Nachtigall, E. G., Zanluchi, A., de Carvalho Myskiw, J., Izquierdo, I., & Furini, C. R. G. (2020). Involvement of medial prefrontal cortex NMDA and AMPA/kainate glutamate receptors in social recognition memory consolidation. *Neurobiology of Learning and Memory*, *168*, 107153. https://doi.org/10.1016/j.nlm.2019.107153

Marmot, M. G., Rose, G., Shipley, M., & Hamilton, P. J. (1978). Employment grade and coronary heart disease in British civil servants. *Journal of Epidemiology and Community Health*, *32*(4), 244–249. https://doi.org/10.1136/jech.32.4.244

Mason, M., Magee, J. C., & Fiske, S. T. (2014). Neural Substrates of Social Status Inference: Roles of Medial Prefrontal Cortex and Superior Temporal Sulcus. *Journal of Cognitive Neuroscience*, *26*(5), 1131–1140. https://doi.org/10.1162/jocn_a_00553

Matsuda, S., Mikawa, S., & Hirai, H. (1999). Phosphorylation of serine-880 in GluR2 by protein kinase C prevents its C terminus from binding with glutamate receptor-interacting protein. *Journal of Neurochemistry*, *73*(4), 1765–1768. https://doi.org/10.1046/j.1471-4159.1999.731765.x

McEwen, B. S. (2007). Physiology and Neurobiology of Stress and Adaptation: Central Role of the Brain. *Physiological Reviews*, *87*(3), 873–904. https://doi.org/10.1152/physrev.00041.2006

Michopoulos, V., Reding, K. M., Wilson, M. E., & Toufexis, D. (2012). Social subordination impairs hypothalamic-pituitary-adrenal function in female rhesus monkeys. *Hormones and Behavior*, *62*(4), 389–399. https://doi.org/10.1016/j.yhbeh.2012.07.014

Milewski, T. M., Lee, W., Young, R. L., Hofmann, H. A., & Curley, J. P. (2024). *Rapid changes in plasma corticosterone and medial amygdala transcriptome profiles during social status change reveal molecular pathways associated with a major life history transition in mouse dominance hierarchies* (p. 2024.05.30.596669). bioRxiv. https://doi.org/10.1101/2024.05.30.596669

Mishra, P., Pandey, C. M., Singh, U., Gupta, A., Sahu, C., & Keshri, A. (2019). Descriptive Statistics and Normality Tests for Statistical Data. *Annals of Cardiac Anaesthesia*, *22*(1), 67–72. https://doi.org/10.4103/aca.ACA_157_18

Mongillo, D. L., Kosyachkova, E. A., Nguyen, T. M., & Holmes, M. M. (2014). Differential effects of chronic fluoxetine on the behavior of dominant and subordinate naked mole-rats. *Behavioural Brain Research*, *258*, 119–126. https://doi.org/10.1016/j.bbr.2013.10.023

Mooney, S. J., Peragine, D. E., Hathaway, G. A., & Holmes, M. M. (2014). A game of thrones: Neural plasticity in mammalian social hierarchies. *Social Neuroscience*, *9*(2), 108–117. https://doi.org/10.1080/17470919.2014.882862

Morgan, D., Grant, K. A., Gage, H. D., Mach, R. H., Kaplan, J. R., Prioleau, O., Nader, S. H., Buchheimer, N., Ehrenkaufer, R. L., & Nader, M. A. (2002). Social dominance in monkeys: Dopamine D2 receptors and cocaine self-administration. *Nature Neuroscience*, *5*(2), Article 2. https://doi.org/10.1038/nn798

Murphy, K. M., Balsor, J., Beshara, S., Siu, C., & Pinto, J. G. A. (2014). A high-throughput semi-automated preparation for filtered synaptoneurosomes. *Journal of Neuroscience Methods*, *235*, 35–40. https://doi.org/10.1016/j.jneumeth.2014.05.036

O'Connell, L. A., & Hofmann, H. A. (2011). The Vertebrate mesolimbic reward system and social behavior network: A comparative synthesis. *Journal of Comparative Neurology*, *519*(18), 3599–3639. https://doi.org/10.1002/cne.22735

Padilla-Coreano, N., Batra, K., Patarino, M., Chen, Z., Rock, R. R., Zhang, R., Hausmann, S. B., Weddington, J. C., Patel, R., Zhang, Y. E., Fang, H.-S., Mishra, S., LeDuke, D. O., Revanna, J., Li, H., Borio, M., Pamintuan, R., Bal, A., Keyes, L. R., … Tye, K. M. (2022). Cortical ensembles orchestrate social competition through hypothalamic outputs. *Nature*, *603*(7902), Article 7902. https://doi.org/10.1038/s41586-022-04507-5

Pallé, A., Zorzo, C., Luskey, V. E., Mcgreevy, K. R., Fernández, S., & Trejo, J. L. (2019). Social dominance differentially alters gene expression in the medial prefrontal cortex without affecting adult hippocampal neurogenesis or stress and anxiety-like behavior. *The FASEB Journal*, *33*(6), 6995–7008. https://doi.org/10.1096/fj.201801600R

Park, M.-J., Seo, B. A., Lee, B., Shin, H.-S., & Kang, M.-G. (2018). Stress-induced changes in social dominance are scaled by AMPA-type glutamate receptor phosphorylation in the medial prefrontal cortex. *Scientific Reports*, *8*(1), Article 1. https://doi.org/10.1038/s41598-018-33410-1

Raleigh, M. J., McGuire, M. T., Brammer, G. L., Pollack, D. B., & Yuwiler, A. (1991). Serotonergic mechanisms promote dominance acquisition in adult male vervet monkeys. *Brain Research*, *559*(2), 181–190. https://doi.org/10.1016/0006-8993(91)90001-C

Redhead, D., & Power, E. A. (2022). Social hierarchies and social networks in humans. *Philosophical Transactions of the Royal Society B: Biological Sciences*, *377*(1845), 20200440. https://doi.org/10.1098/rstb.2020.0440

Richardson, J. T. E. (2011). Eta squared and partial eta squared as measures of effect size in educational research. *Educational Research Review*, *6*(2), 135–147. https://doi.org/10.1016/j.edurev.2010.12.001

Šabanović, M., Liu, H., Mlambo, V., Aqel, H., & Chaudhury, D. (2020). What it takes to be at the top: The interrelationship between chronic social stress and social dominance. *Brain and Behavior*, *10*(12). Scopus. https://doi.org/10.1002/brb3.1896

Sander, H., Wallace, S., Plouse, R., Tiwari, S., & Gomes, A. V. (2019). Ponceau S Waste: Ponceau S Staining for Total Protein Normalization. *Analytical Biochemistry*, *575*, 44–53. https://doi.org/10.1016/j.ab.2019.03.010

Sapolsky, R. M. (2004). Social Status and Health in Humans and Other Animals. *Annual Review of Anthropology*, *33*(1), 393–418. https://doi.org/10.1146/annurev.anthro.33.070203.144000

Sapolsky, R. M. (2005). The Influence of Social Hierarchy on Primate Health. *Science*, *308*(5722), 648–652. https://doi.org/10.1126/science.1106477

Scorrano, F., Carrasco, J., Pastor-Ciurana, J., Belda, X., Rami-Bastante, A., Bacci, M. L., & Armario, A. (2015). Validation of the long-term assessment of hypothalamic-pituitary-adrenal activity in rats using hair corticosterone as a biomarker. *The FASEB Journal*, *29*(3), 859–867. https://doi.org/10.1096/fj.14-254474

Seamans, J. K., Lapish, C. C., & Durstewitz, D. (2008). Comparing the prefrontal cortex of rats and primates: Insights from electrophysiology. *Neurotoxicity Research*, *14*(2), 249–262. https://doi.org/10.1007/BF03033814

Sheldon, A. L., & Robinson, M. B. (2007). The Role of Glutamate Transporters in Neurodegenerative Diseases and Potential Opportunities for Intervention. *Neurochemistry International*, *51*(6–7), 333–355. https://doi.org/10.1016/j.neuint.2007.03.012

Sheng, M., & Hoogenraad, C. C. (2007). The Postsynaptic Architecture of Excitatory Synapses: A More Quantitative View. *Annual Review of Biochemistry*, *76*(1), 823–847. https://doi.org/10.1146/annurev.biochem.76.060805.160029

Shepherd, J. D., & Huganir, R. L. (2007). The cell biology of synaptic plasticity: AMPA receptor trafficking. *Annual Review of Cell and Developmental Biology*, *23*, 613–643. Scopus. https://doi.org/10.1146/annurev.cellbio.23.090506.123516

Shively, C. A., Register, T. C., & Clarkson, T. B. (2009). Social Stress, Visceral Obesity, and Coronary Artery Atherosclerosis: Product of a Primate Adaptation. *American Journal of Primatology*, *71*(9), 742–751. https://doi.org/10.1002/ajp.20706

Smith-Osborne, L., Duong, A., Resendez, A., Palme, R., & Fadok, J. P. (2023). Female dominance hierarchies influence responses to psychosocial stressors. *Current Biology : CB*, *33*(8), 1535-1549.e5. https://doi.org/10.1016/j.cub.2023.03.020

Snyder-Mackler, N., Burger, J. R., Gaydosh, L., Belsky, D. W., Noppert, G. A., Campos, F. A., Bartolomucci, A., Yang, Y. C., Aiello, A. E., O'Rand, A., Harris, K. M., Shively, C. A., Alberts, S. C., & Tung, J. (2020). Social determinants of health and survival in humans and other animals. *Science*, *368*(6493), eaax9553. https://doi.org/10.1126/science.aax9553

Strauss, E. D., Curley, J. P., Shizuka, D., & Hobson, E. A. (2022). The centennial of the pecking order: Current state and future prospects for the study of dominance hierarchies. *Philosophical Transactions of the Royal Society B: Biological Sciences*, *377*(1845), 20200432. https://doi.org/10.1098/rstb.2020.0432

Strauss, E. D., & Shizuka, D. (2022). The dynamics of dominance: Open questions, challenges and solutions. *Philosophical Transactions of the Royal Society B: Biological Sciences*, *377*(1845), 20200445. https://doi.org/10.1098/rstb.2020.0445

Tada, H., Miyazaki, T., Takemoto, K., Takase, K., Jitsuki, S., Nakajima, W., Koide, M., Yamamoto, N., Komiya, K., Suyama, K., Sano, A., Taguchi, A., & Takahashi, T. (2016). Neonatal isolation augments Social dominance by altering actin dynamics in the medial prefrontal cortex. *Proceedings of the National Academy of Sciences of the United States of America*, *113*(45), E7097–E7105. Scopus. https://doi.org/10.1073/pnas.1606351113

Tan, H. L., Chiu, S.-L., Zhu, Q., & Huganir, R. L. (2020). GRIP1 regulates synaptic plasticity and learning and memory. *Proceedings of the National Academy of Sciences*, *117*(40), 25085–25091. https://doi.org/10.1073/pnas.2014827117

Terashima, A., Cotton, L., Dev, K. K., Meyer, G., Zaman, S., Duprat, F., Henley, J. M., Collingridge, G. L., & Isaac, J. T. R. (2004). Regulation of Synaptic Strength and AMPA Receptor Subunit Composition by PICK1. *The Journal of Neuroscience*, *24*(23), 5381–5390. https://doi.org/10.1523/JNEUROSCI.4378-03.2004

Thacker, J. S., Yeung, D. H., Staines, W. R., & Mielke, J. G. (2016). Total protein or high-abundance protein: Which offers the best loading control for Western blotting? *Analytical Biochemistry*, *496*, 76–78. https://doi.org/10.1016/j.ab.2015.11.022

Thanos, P. K., Cavigelli, S. A., Michaelides, M., Olvet, D. M., Patel, U., Diep, M. N., & Volkow, N. D. (2009). A Non-Invasive Method for Detecting the Metabolic Stress Response in Rodents: Characterization and Disruption of the Circadian Corticosterone Rhythm. *Physiological Research / Academia Scientiarum Bohemoslovaca*, *58*(2), 219–228.

Tibbetts, E. A., Pardo-Sanchez, J., & Weise, C. (2022). The establishment and maintenance of dominance hierarchies. *Philosophical Transactions of the Royal Society B: Biological Sciences*, *377*(1845), 20200450. https://doi.org/10.1098/rstb.2020.0450

van den Berg, W. E., Lamballais, S., & Kushner, S. A. (2015). Sex-Specific Mechanism of Social Hierarchy in Mice. *Neuropsychopharmacology*, *40*(6), Article 6. https://doi.org/10.1038/npp.2014.319

Varholick, J. A., Pontiggia, A., Murphy, E., Daniele, V., Palme, R., Voelkl, B., Würbel, H., & Bailoo, J. D. (2019). Social dominance hierarchy type and rank contribute to phenotypic variation within cages of laboratory mice. *Scientific Reports*, *9*(1), Article 1. https://doi.org/10.1038/s41598-019-49612-0

Villasana, L. E., Klann, E., & Tejada-Simon, M. V. (2006). Rapid isolation of synaptoneurosomes and postsynaptic densities from adult mouse hippocampus.

Journal of Neuroscience Methods, *158*(1), 30–36. https://doi.org/10.1016/j.jneumeth.2006.05.008

Voisin, D. A., Wakeford, A., Nye, J., Mun, J., Jones, S. R., Locke, J., Huhman, K. L., Wilson, M. E., Albers, H. E., & Michopoulos, V. (2022). Sex and social status modify the effects of fluoxetine on socioemotional behaviors in Syrian hamsters and rhesus macaques. *Pharmacology Biochemistry and Behavior*, *215*, 173362. https://doi.org/10.1016/j.pbb.2022.173362

Wang, F., Kessels, H. W., & Hu, H. (2014). The mouse that roared: Neural mechanisms of social hierarchy. *Trends in Neurosciences*, *37*(11), 674–682. https://doi.org/10.1016/j.tins.2014.07.005

Wang, F., Zhu, J., Zhu, H., Zhang, Q., Lin, Z., & Hu, H. (2011). Bidirectional Control of Social Hierarchy by Synaptic Efficacy in Medial Prefrontal Cortex. *Science*, *334*(6056), 693–697. https://doi.org/10.1126/science.1209951

Williamson, C. M., Klein, I. S., Lee, W., & Curley, J. P. (2019). Immediate early gene activation throughout the brain is associated with dynamic changes in social context. *Social Neuroscience*, *14*(3), 253–265. https://doi.org/10.1080/17470919.2018.1479303

Williamson, C. M., Lee, W., & Curley, J. P. (2016). Temporal dynamics of social hierarchy formation and maintenance in male mice. *Animal Behaviour*, *115*, 259–272. https://doi.org/10.1016/j.anbehav.2016.03.004

Williamson, C. M., Lee, W., DeCasien, A. R., Lanham, A., Romeo, R. D., & Curley, J. P. (2019). Social hierarchy position in female mice is associated with plasma corticosterone levels and hypothalamic gene expression. *Scientific Reports*, *9*(1), Article 1. https://doi.org/10.1038/s41598-019-43747-w

Williamson, C. M., Lee, W., Romeo, R. D., & Curley, J. P. (2017). Social context-dependent relationships between mouse dominance rank and plasma hormone levels. *Physiology & Behavior*, *171*, 110–119. https://doi.org/10.1016/j.physbeh.2016.12.038

Windle, R. J., Wood, S. A., Shanks, N., Lightman, S. L., & Ingram, C. D. (1998). Ultradian Rhythm of Basal Corticosterone Release in the Female Rat: Dynamic Interaction with the Response to Acute Stress*. *Endocrinology*, *139*(2), 443–450. https://doi.org/10.1210/endo.139.2.5721

Yamaguchi, Y., Lee, Y.-A., Kato, A., Jas, E., & Goto, Y. (2017). The roles of dopamine D2 receptor in the social hierarchy of rodents and primates. *Scientific Reports*, *7*. Scopus. https://doi.org/10.1038/srep43348

Yin, Y.-Y., Lai, Z.-K., Yan, J.-Z., Wei, Q.-Q., Wang, B., Zhang, L.-M., & Li, Y.-F. (2023). The interaction between social hierarchy and depression/anxiety: Involvement of glutamatergic pyramidal neurons in the medial prefrontal cortex (mPFC). *Neurobiology of Stress*, *24*. Scopus. https://doi.org/10.1016/j.ynstr.2023.100536

Zhou, T., Zhu, H., Fan, Z., Wang, F., Chen, Y., Liang, H., Yang, Z., Zhang, L., Lin, L., Zhan, Y., Wang, Z., & Hu, H. (2017). History of winning remodels thalamo-PFC circuit to

reinforce social dominance. *Science*, *357*(6347), 162–168. https://doi.org/10.1126/science.aak9726

Zhu, J. J., Qin, Y., Zhao, M., Van Aelst, L., & Malinow, R. (2002). Ras and Rap control AMPA receptor trafficking during synaptic plasticity. *Cell*, *110*(4), 443–455. https://doi.org/10.1016/s0092-8674(02)00897-8